Journal of Inorganic Biochemistry 145 (2015) 108–120

Contents lists available at ScienceDirect

Journal of Inorganic Biochemistry

journal homepage: www.elsevier.com/locate/jinorgbio

Heteroditopic P,N ligands in gold(I) complexes: Synthesis, structure and cytotoxicity

Telisha Traut-Johnstone [a,b], Stonard Kanyanda [c,1], Frederik H. Kriel [b], Tanya Viljoen [a], P.D. Riekert Kotze [a], Werner E. van Zyl [a,d], Judy Coates [b,2], D. Jasper G. Rees [c,3], Mervin Meyer [c], Raymond Hewer [b], D. Bradley G. Williams [a,e,*]

[a] Research Centre for Synthesis and Catalysis, Department of Chemistry, University of Johannesburg, P.O. Box 524, Auckland Park 2006, South Africa
[b] Advanced Materials Division, Mintek, 200 Malibongwe Drive, Strijdom Park 2125, South Africa
[c] Department of Biotechnology, University of the Western Cape, Private Bag X17, Bellville, Cape Town 7535, South Africa
[d] School of Chemistry and Physics, University of KwaZulu-Natal, Westville Campus, Private Bag X54001, Durban, 4000, South Africa
[e] Ferrier Research Institute, Victoria University of Wellington, 69 Gracefield Rd, Lower Hutt 5010, New Zealand

ARTICLE INFO

Article history:
Received 8 October 2014
Received in revised form 20 January 2015
Accepted 21 January 2015
Available online 30 January 2015

Keywords:
Gold(I) complexes
Metal-based drugs
P,N ligands
Cytotoxicity

ABSTRACT

New heteroditopic, bi- and multidentate imino- and aminophosphine ligands were synthesised and complexed to [AuCl(THT)] (THT = tetrahydrothiophene). X-ray crystallography confirmed Schiff base formation in three products, the successful reduction of the imino-group to the sp^3-hybridised amine in several instances, and confirmed the formation of mono-gold(I) imino- and aminophosphine complexes for four Au-complexes. Cytotoxicity studies in cancerous and non-cancerous cell lines showed a marked increase in cytotoxicity upon ligand complexation to gold(I). These findings were supported by results from the 60-cell line fingerprint screen of the Developmental Therapeutics Programme of the National Institutes of Health for two promising compounds. The cytotoxicity of some of these ligands and gold(I)complexes is due to the induction of apoptosis. The ligands and gold(I)complexes demonstrated selective toxicity towards specific cell lines, with Jurkat T cells being more sensitive to the cytotoxic effects of these compounds, while the non-cancerous human cell line KMST6 proved more resistant when compared to the cancerous cell lines. Results from the NIH DTP 60 cell-line fingerprint screen support the observed enhancement of cytotoxicity upon gold(I) complexation. One gold(I)complex induced high levels of apoptosis at concentrations of 50 μM in all the cell lines screened in this study, while some of the other compounds selectively induced apoptosis in the cell lines. These results point towards the potential for selective toxicity to cancerous cells through the induction of apoptosis.

1. Introduction

The recent interest in the biochemistry and bio-inorganic chemistry of gold has triggered a flood of reports on the use of gold complexes as potential treatment for a variety of disease models, including rheumatoid arthritis [1–3] and other chronic inflammatory and auto-immune diseases [4–6], various cancers [7–10], as well as bacterial, fungal and viral infections [11–13]. Most of these reports focus on gold in either +I or +III oxidation states, as these forms are comparatively stable in aqueous solution, facilitating their use in biological research [14–16]. Several gold compounds are in clinical for the treatment of rheumatoid arthritis [17,18]. Gold(I) mostly forms linear, two-coordinate complexes with so-called "soft" ligands such as sulfur and phosphorus [19,20]. Conversely, gold(III) is isoelectronic with Pt(II) and typically forms square-planar, 4-coordinate complexes [21,22]. Due to this similarity, many gold(III) complexes have been synthesised and tested as analogues for Pt(II) drugs such as the highly effective anticancer drug cisplatin [23,24]. Despite their structural similarities, different mechanisms of biological action for gold(III) and platinum(II) complexes have been proposed. While platinum(II) complexes have been shown to intercalate into DNA strands, inhibiting the function of various DNA and RNA enzymes [25], the mode of action of gold(I) and gold(III) complexes has not been conclusively determined. Recent studies have indicated that the cytotoxic anti-cancer mechanisms of gold complexes appear to be distinct from cisplatin and unrelated to DNA intercalation [26,27]. Several mechanisms have been proposed that involve protein inhibition and/or interaction [27–32], and involve the induction of cellular apoptosis via alterations to the intracellular mitochondrial membrane potential, stimulating the release of pre-apoptotic factors and the subsequent downstream activation of caspases [33].

* Corresponding author at: Ferrier Research Institute, Victoria University of Wellington, 69 Gracefield Rd, Lower Hutt 5010, New Zealand.
E-mail addresses: bwilliams@uj.ac.za, Bradley.williams@vuw.ac.nz (D.B.G. Williams).
[1] Deceased.
[2] Present address: Technology Innovation Agency, P.O Box 172, Pretoria 0063, South Africa.
[3] Present address: Biotechnology Platform, Agricultural Research Council, Private Bag X05, Onderstepoort 0110, South Africa.

http://dx.doi.org/10.1016/j.jinorgbio.2015.01.014
0162-0134/

Heteroditopic multidentate P,N ligands [34–37] show differential binding ability between the P and N atoms, a characteristic put to use in homogeneous catalysts [38–40]. Investigations into the structure and reactivity of this class of compounds have intensified, including their potential use in various medicinal applications such as anticancer activity [41, 42]. The complexation of P,N ligands to transition metals such as Pd(II) and Pt(II) centres has been well studied. However, similar investigations into the gold(I) complexation of the P,N ligand class are limited [43]. We have previously communicated the differential gold(I) binding affinity of the P and N donor atoms in bi- and multidentate bi-metallic binding systems [44], where the reactivity of the ligand may be tailored for specific applications. As a part of our continued interest in the field of coordination complexes and their applications [45], a range of new bi- and multidentate heteroditopic P,N ligands has been prepared representing the nitrogen in both sp^2 and sp^3 hybridisation states. The complexation of the ligands to monovalent gold(I) and the structures of the resultant imino- and aminophosphine gold(I) complexes were investigated with the aid of single crystal X-ray analysis. In this paper, we report on the synthesis, structure evaluation and promising in vitro cytotoxicity profiles observed for a family of fifteen structurally related imino- and aminophosphine P,N ligands and their corresponding gold(I) complexes in a panel of thirteen cell lines which includes ten human cancer cell lines and one non-cancerous human cell line and two rodent cell lines. Furthermore, we demonstrate the selective cytotoxicity displayed by the compound family towards cancerous cell lines over the non-cancerous human cell line KMST6, as well as the enhanced cytotoxic potential demonstrated upon complexation of the free ligands to the gold(I) metal centre. Finally, we report on the results obtained for two compounds (one ligand and one gold(I)complex) screened through the 60-cell line fingerprint screen of the Developmental Therapeutics Program (DTP) of the National Institutes of Health (NIH).

2. Results and discussion

2.1. Synthesis

With our previous work as a springboard [44], we synthesised a collection of P,N ligands and their corresponding gold(I) complexes with the general structures **2** and **3**, respectively (Fig. 1). The amine starting materials were chosen so that a diverse series of products could be generated based on R-group structure, with some measure of series correlation between the products. Synthesis of the P,N ligand library was accomplished by coupling a variety of primary amines with 2-(diphenylphosphino)benzaldehyde (**1**) in a Schiff base condensation reaction facilitated by the azeotropic removal of water from the system (Scheme 1). This strategy allowed the one-pot synthesis of iminophosphine ligands **4**–**12** as well as their reduced aminophosphine counterparts **13**–**19**. Accordingly, 1 equivalent of aldehyde **1** was reacted with 1.1 M equivalents of amine in toluene under reflux and the product purified by employing Kugel–Rohr bulb-to-bulb vacuum distillation. The purification of the iminophosphine ligands was performed under an inert (nitrogen) atmosphere to prevent the oxidation of the P atom, preserving its metal-binding affinity. A reduction step using 1.1 equivalents of sodium borohydride in methanol was required to obtain the aminophosphine ligands. Ligands obtained from either of

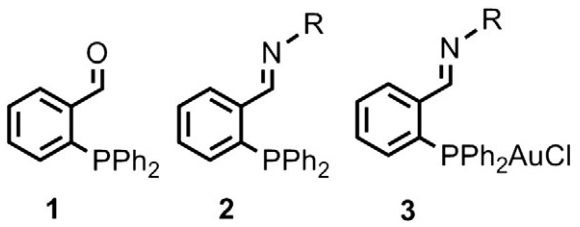

Fig. 1. Structural backbone of the P,N ligands and corresponding gold(I) complexes.

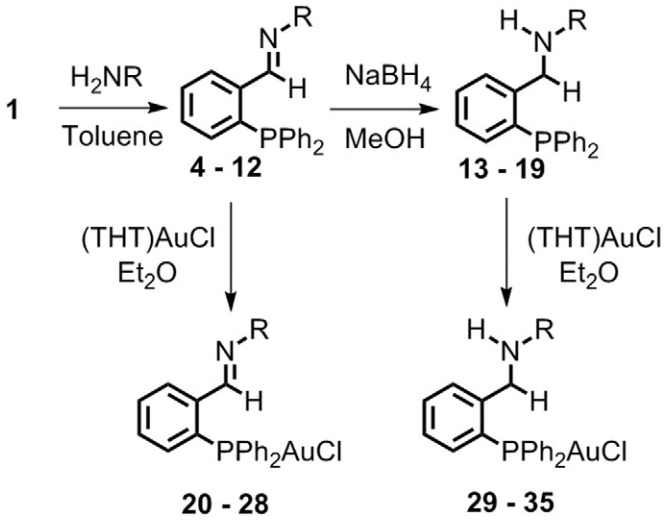

Scheme 1. Facile one-pot synthesis and gold(I) complexation of imino- and aminophosphine ligands. **4**: R = methyl; **5**, **20**: R = butyl; **6**, **13**, **22**, **29**: R = benzyl; **7**, **14**, **23**, **30**: R = phenyl; **8**, **15**, **24**, **31**: R = isopropyl; **9**, **17**, **25**, **33**: R = 2-pyridylethyl; **10**, **18**, **26**, **34**: R = 3-dimethylamino-propyl; **11**, **19**, **27**, **35**: R = 2-thiophenethyl; **12**, **28**: R = *tert*-butyl; **16**, **32**: R = 2-pyridylmethyl; **21**: R = phenylethyl.

these steps complexed to the gold(I) starting material in a similar way as observed for the gold(I) complexation of triphenylphosphine (**36**; Scheme 2B) [46], resulting in the corresponding P,N gold(I) complexes **20**–**35** (Scheme 2A). The ^{1}H NMR spectra of the imine ligands **4**–**12** display a characteristic doublet signal for the imine-H group at around 8.7–8.9 ppm with $J_{H,P}$ = 4.2–5.4 Hz, accompanied by a ^{13}C NMR signal at 154–161 ppm with $J_{C,P}$ = 20.4–22.4 Hz and a ^{31}P NMR signal at around −13 ppm. In contrast, the amine ligands **13**–**19** show a diagnostic benzylic CH_2 moiety in the ^{1}H NMR spectra, which presents as a two proton singlet at 3.9–4.4 ppm, accompanied by a ^{13}C NMR signal presenting as a doublet at 47.0–52.4 ppm with $J_{C,P}$ = 20.6–23.5 Hz, while the ^{31}P NMR spectrum is characterised by a shifted signal at around −16 ppm. The main feature differentiating the free ligands from their gold(I) complexes is the signals in the ^{31}P NMR spectra, which shift significantly downfield to 30.8–32.6 ppm for P,imine complexes **20**–**18** and to 25.7–26.3 ppm for P,amine complexes **29**–**35**.

2.2. Structural analysis

2.2.1. Crystallography of ligands *4* and *14*

Several X-ray crystal structures were obtained to confirm the proposed structure, in agreement with related studies [47]. Specifically,

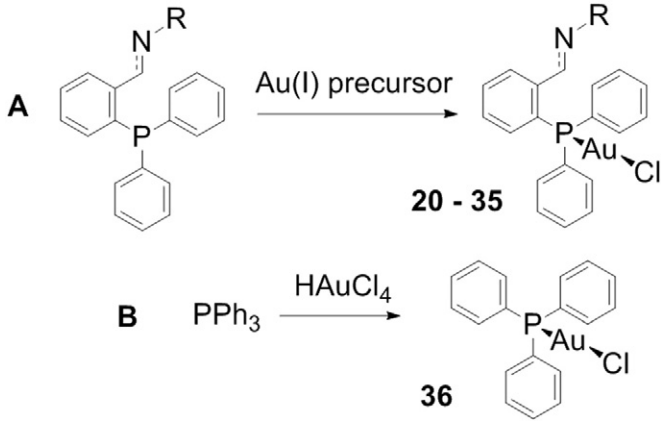

Scheme 2. A: Gold(I) complexation of imino- and aminophosphine ligands to afford the corresponding gold(I) complexes **20**–**35**. B: Binding mode reported for (triphenylphosphine)gold(I) chloride **36** [33].

we report here single crystal analysis that represents each of the four product types explored in our synthesis: iminophosphine ligands; aminophosphine ligands; iminophosphine gold(I) complexes and aminophosphine gold(I) complexes. The single crystal structure obtained for iminophosphine ligand **4** (Fig. 2) confirmed the proposed Schiff base condensation between C17 of 2-(diphenylphosphino)benzaldehyde and N1 of the primary amine, methylamine (C–N bond length of 1.246(3) Å). The hydrogen atoms riding on C18 show some disorder about the freely rotating methylamine single bond between N1 and C18. The molecular packing shows reciprocal hydrogen bonding between N1 and H26 (2.662 Å) of two adjacent molecule pairs of **4** (Supplementary Fig. S1). In the single crystal structure obtained for aminophosphine ligand **14** (Fig. 3), the most obvious feature was the reduced single bond between N1 and C37. The bond length of 1.486(11) Å is typical of singly bonded C–N species (C═N bonds are typically in the order of 1.2 Å, as illustrated for iminophosphine ligand **4**). This is clear evidence that the reduction of the original iminophosphine ligands proceeds to yield the corresponding range of aminophosphine ligands.

*2.2.2. Crystallography of gold complexes **21**, **23**, **30a** and **30b***

Gold(I) complexation facilitated the formation of suitable single crystals and several examples of both imino- and aminophosphine gold(I) complexes were obtained. In all cases mono-gold(I) complexes resulted with the P–Au–Cl bond angle approaching linearity, falling in the range 175.5–179.6° (Table 1). In the crystal structures of iminophosphine gold(I) complexes **21** and **23**, we not only confirmed the proposed bond formation between the P and Au(I) atoms (Figs. 4 and 5) but the characteristic C═N double bond was also evident in these structures. The structure of **21** (Fig. 4) shows some disorder of the flexible phenylethyl moiety, due mainly to the inherent flexibility of the aliphatic carbon chain. The molecular packing shows the formation of reciprocal H–Cl short contacts between Cl1 and H35 (2.858 Å) and Cl1 and H37 (2.903 Å) of two adjacent molecule pairs of **21**, respectively, as well as demonstrating a third hydrogen–chloride short contact between Cl1 and H24 (2.924 Å) of a third molecule (Supplementary Fig. S2). The crystal packing also illustrates the head-to-head staggered aromatic stacking interactions between the disordered phenylethyl moieties of two adjacent molecules of **21**. A similar three pronged hydrogen–chloride short contact network (Supplementary Fig. S3) was noted in the single crystal structure of **23** (Fig. 5), with two H–Cl short contacts forming between Cl1 and H33 (2.869 Å) and Cl1 and H34 (2.918 Å) on an adjacent molecule, respectively, while the third short contact can be observed between Cl1 and H50A (2.580 Å) located on a disordered dichloromethane molecule.

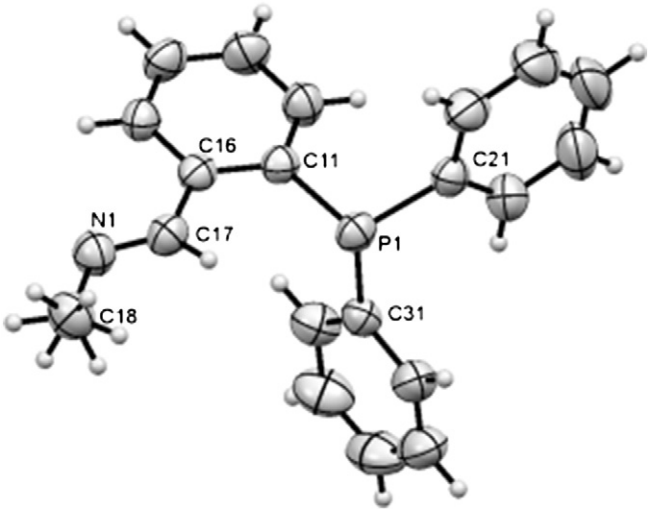

Fig. 2. ORTEP diagram of the crystal structure obtained for iminophosphine ligand **4**, drawn with 50% probability ellipsoids. Disorder of the hydrogens on C20 is displayed.

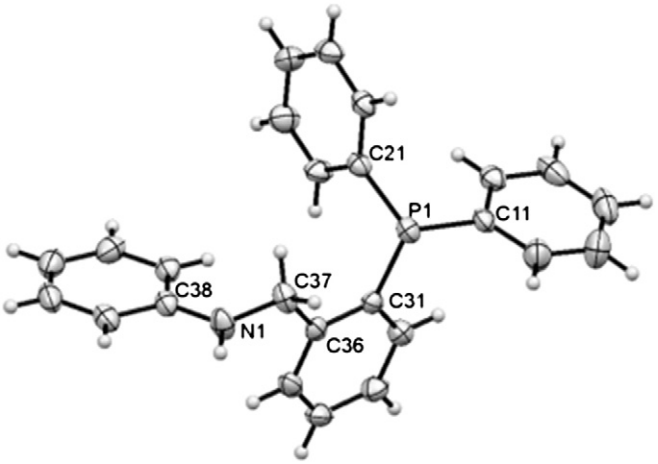

Fig. 3. ORTEP diagram of the crystal structure obtained for aminophosphine ligand **14**, drawn with 50% probability ellipsoids.

Crystallisation of aminophosphine gold(I) complex **30** afforded two different structures (Figs. 6 and 7), depending on the processing to which the compound had been subjected. While **30a** crystallised as the neutral gold(I) complex from a layered solution of diethyl ether and hexane, **30b** crystallised as the hydrochloride salt derivative from a layered solution of chloroform and *n*-heptane. Compound **30b** had been recovered from an aqueous HCl-acidified solution of **30a**. Although the crystal structures of **30a** and **30b** show considerable differences in terms of the interaction networks formed and the packing of the respective crystals, both crystals clearly displayed the reduced single bond C–N that is characteristic of the aminophosphine ligands, as discussed for ligand **14**. In addition, both aminophosphine gold(I) complexes exhibited exclusively mono-gold(I) structures and adopted the linear geometry expected, with P–Au–Cl bond angles showing only slight distortion from linearity (176.77° and 175.48° for **30a** and **30b**, respectively). Furthermore, Au–P and Au–Cl bond lengths are in good agreement with the corresponding bond lengths reported for **36** [AuCl(PPh$_3$)] (Table 1; Figs. 6 and 7). Complex **30a** (Fig. 6) crystallised as the neutral aminophosphine gold(I) complex without any solvent inclusion. The structure of **30a** displays one reciprocal HCl short contact between Cl1 of the AuCl moiety and H15 (2.714 Å) of an adjacent molecule (Supplementary Fig. S4). Complex **30b** (Fig. 7) crystallised as its hydrochloride salt with the inclusion of two chloroform solvent molecules. In contrast to the simple crystal packing observed for **30a**, an elaborate network of interactions is formed between adjacent molecules of **30b** and the solvent-derived chloroform molecules (Supplementary Fig. S5). Specifically, Cl5 forms intramolecular hydrogen–chloride interactions with H1B (2.214 Å) situated on the positively charged N1, and intermolecular interactions with H1A (2.176 Å) situated on the positively charged N1 of an adjacent molecule. A third hydrogen–chloride short contact can be observed between Cl5 and H50 (2.687 Å) situated on one of the solvent-derived chloroform molecules. Furthermore, an intermolecular

Table 1
Comparison of selected bond angles (°) and bond lengths (Å) observed in prepared compounds and [AuClPPh$_3$], compound 36.

Crystal	Bond angle	Bond lengths (Å)		
	P–Au–Cl (°)	N–C	Au–P	Au–Cl
4	N/A	1.246(3)	N/A	N/A
14	N/A	1.486(11)	N/A	N/A
21	177.33(3)	1.257(5)	2.239(1)	2.295(1)
23	177.81(3)	1.278(5)	2.236(1)	2.295(1)
30a	175.48(4)	1.426(8)	2.228(2)	2.279(2)
30b	176.77(4)	1.486(11)	2.239(2)	2.281(2)
36	179.63(8)	N/A	2.23(5)	2.27(9)

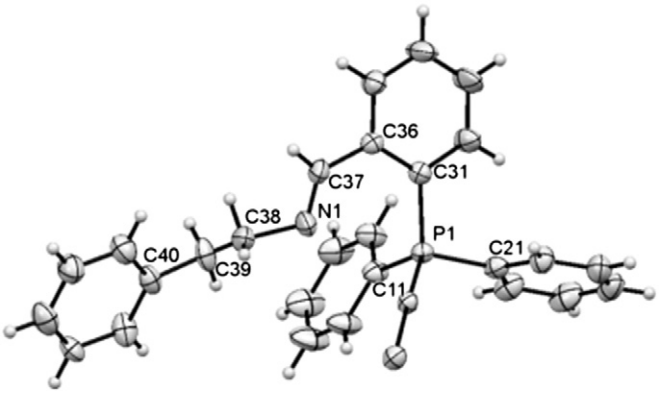

Fig. 4. ORTEP diagram of the crystal structure obtained for iminophosphine gold(I) complex **21**, drawn with 50% probability ellipsoids. Disorder of the phenylethyl moiety has been omitted for clarity.

chloride–chloride short contact can be distinguished between Cl5 and Cl2 of two separate solvent derived chloroform molecules (3.316 Å). The chloride from the AuCl moiety participates in an intermolecular hydrogen–chloride short contact between Cl1 and H15 (2.949 Å) of an adjacent molecule (similar to the interaction observed in the crystal structure of **30a**), as well as forming a chloride–chloride short contact between Cl1 and Cl4 (3.401 Å) situated on a solvent-derived chloroform molecule (Supplementary Fig. S6). In the crystallography, some level A and B alerts remain. These stem from residual electron density present around the gold atoms present in the structures. Absorption corrections have been made to compensate for most of the electron density of gold, but these have been unable to compensate completely for the electron density of the heavy gold element and thus the "unaccounted" for electron density around the gold atoms still present as level A and B alerts.

2.3. In vitro evaluation of cytotoxicity

Four closely related iminophosphine gold(I) complexes were shown recently to have low micro-molar in vitro anticancer activity against the human oesophageal cancer cell lines WHCO1 and KYSE450 as measured via the 3-(4,5-dimethylthiazol-2-yl)-2,5-diphenyltetrazolium bromide (MTT) colorimetric assay [48]. No similar results have been reported for the P,N ligands or aminophosphine gold(I) complexes. It was therefore of interest to evaluate the activity of our varied family of P,N ligands

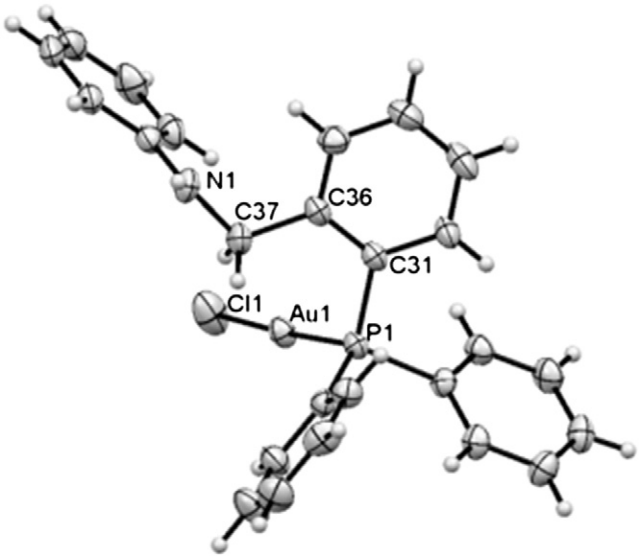

Fig. 6. ORTEP diagram of the crystal structure obtained for aminophosphine gold(I) complex **30a**, drawn with 50% probability ellipsoids.

and their corresponding gold(I) P,N complexes in a more extensive range of cell lines, both cancerous and non-cancerous. In this study the cytotoxic effects of the ligands and their corresponding gold(I) complexes were evaluated on a panel of thirteen cell lines. This study was performed on ten cancerous human cell lines (A549J, Caski, HepG2, HeLa, HT29, H157, Jurkat T, MCF7, MG-63 and Hek293T), one non-cancerous human cell line (KMST6) and two non-cancerous rodent cell lines (CHO and NIH 3T3). Two in vitro bioassays (the MTT colorimetric endpoint assay [49–53] and the APOP*ercentage*™ apoptosis assay [54]) were used to assess cytotoxic effects of the thirty compounds.

The MTT assay was used to determine the IC_{50} values for all thirty compounds on the thirteen cell lines used in this study. The IC_{50} values for the positive control, cisplatin, were more than 100 μM for all the cell lines tested in this study. For the purposes of the MTT cytotoxicity assay, compounds with IC_{50} values of 50 μM or lower were considered to be biologically active. In comparing the cytotoxic potential of the free ligands (Table 2) and the gold(I) complexes (Table 3), it is immediately evident that a generally higher level of cell lethality resulted from the inclusion of gold to the ligand system, in line with previously published reports [55,56]. Furthermore, the cytotoxicity results of the most active

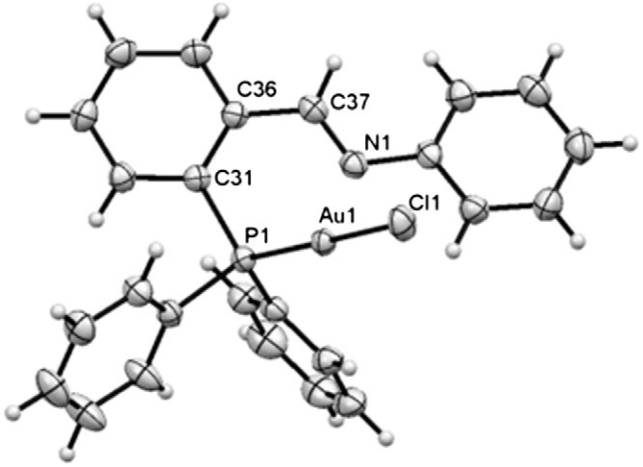

Fig. 5. ORTEP diagram of the crystal structure obtained for iminophosphine gold(I) complex **23**, drawn with 50% probability ellipsoids. The dichloromethane molecule has been omitted for clarity.

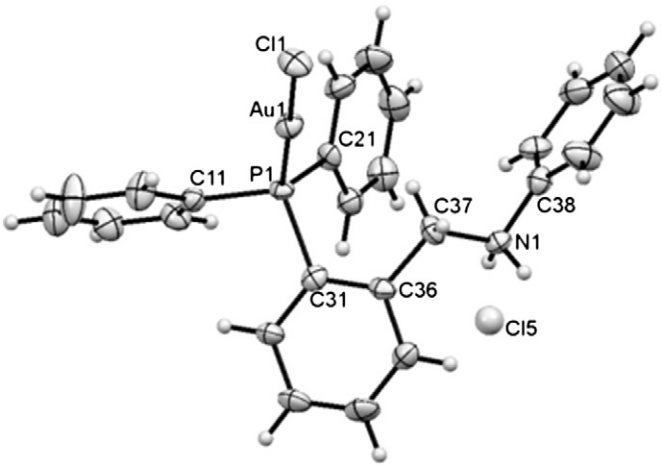

Fig. 7. ORTEP diagram of the crystal structure obtained for aminophosphine gold(I) complex **30b**, drawn at a 50% probability level. The chloroform molecules have been omitted for clarity.

Table 2
Summary of the cytotoxic IC_{50} values (μM) after treatment with P,N ligands.[a]

Sample	KMST6	A549J	Caski	HepG2	HeLa	HT29	H157	Hek293T	Jurkat T	MCF7	MG63	CHO	3T3
5	‡	‡	‡	‡	‡	‡	‡	‡	‡	‡	‡	‡	‡
6	‡	‡	‡	‡	‡	‡	‡	90	‡	‡	‡	‡	‡
7	75	‡	‡	‡	35	‡	28	<10	<10	‡	50	‡	‡
8	‡	‡	‡	‡	‡	‡	‡	20	‡	‡	‡	‡	‡
9	‡	‡	‡	‡	‡	‡	‡	90	25	‡	‡	‡	‡
10	‡	‡	‡	‡	‡	‡	‡	50	80	‡	‡	‡	50
11	‡	‡	‡	98	‡	‡	‡	20	80	‡	‡	‡	20
12	‡	‡	‡	‡	‡	‡	‡	20	‡	‡	‡	‡	20
13	‡	‡	‡	95	95	‡	‡	10	80	‡	‡	‡	‡
14	35	35	55	‡	‡	48	‡	30	10	35	‡	35	‡
15	70	‡	‡	‡	‡	‡	‡	50	‡	50	‡	‡	‡
16	‡	‡	‡	50	‡	‡	‡	‡	‡	‡	‡	‡	‡
17	95	‡	‡	‡	‡	‡	‡	10	‡	‡	15	85	18
18	‡	‡	‡	‡	98	‡	‡	50	20	‡	‡	‡	‡
19	95	‡	‡	35	95	‡	‡	10	35	‡	‡	80	35

[a] ‡ indicates an IC_{50} of more than 100 μM; values reported are the average of at least triplicate experiments and standard deviations did not exceed 5%. The IC_{50} values for the positive control, cisplatin, were more than 100 μM for all the cell lines tested in this study.

gold(I) complexes detailed here correspond well to the findings reported for three recent studies on gold(I) cytotoxicity [57–59], with IC_{50} values in the low- to sub-micromolar range. While the free P,N ligands showed cytotoxic IC_{50} values under 50 μM in 26 of the 195 assays, the gold(I) complexes proved much more toxic, with IC_{50} values below 50 μM in 105 of the 195 assays performed. Based on the MTT assay, **14** was more cytotoxic compared to the other ligands, while **5** and **6** demonstrated the lowest cytotoxicity. The IC_{50} value for **14** was less than 50 μM in seven of the cell lines tested in this study, while the IC_{50} values for **5** and **6** were higher than 50 μM in all cell lines screened in this study. In general, Hek293T cells were more sensitive to the effects of ligands, while Caski cells were more resistant. The IC_{50} values for nine of the ligands were below 50 μM in Hek293T cells, while the IC_{50} values for all the ligands were higher than 50 μM in Caski cells. Based on the MTT assay, **22**, **29** and **35** were the most cytotoxic gold(I) complexes, while **30** demonstrated the lowest cytotoxicity. The IC_{50} value for **22**, **29** and **35** was below 50 μM in twelve of the cell lines tested in this study, while the IC_{50} values for **30** were higher than 50 μM in twelve of the cell lines screened in this study. Nine of the gold(I) complexes (**22**, **23**, **26**, **27**, **29**, **30**, **33**, **34** and **35**) had IC_{50} values below 10 μM at least one cell line. This is consistent with values obtained for platinum(II) and gold(I) iminophosphine complexes in a related study [48]. In other work [60], Auranofin was found to have activity against MCF7 cells with an IC_{50} value of 11.4 μM. In the present study, the Hek293T cell line was overall more sensitive to the effects of gold(I) complexes, while the Caski cell line was the most resistant cell line.

Given the low activity of the ligands, no structure–activity analysis was performed. For the gold complexes, overall, the amines tended to be more active than the imines. Nevertheless, within the imines, simple aliphatic R groups tended to lower activity. More notable activity was achieved with R = phenyl (**23**), 3-dimethylaminopropyl (**26**) and 2-thiophenylethyl (**27**) substituents, these giving IC_{50} values of ≤15 μM in three or more cell lines. Particularly good activity was achieved with **26** and **27**, with IC_{50} values of ≤10 μM in three cell lines each. Of these, there was overlap in the HT29 cell line and in the Hek293T cell line. For the amines, aromatic functionality tended to improve activity. Most notable activity was identified for R = benzyl (**29**), phenyl (**30**), 2-pyridylethyl (**33**) and 2-thiophenylethyl (**35**), all of which contain aromatic functional groups. Interestingly, compound **34** with its 3-dimethylaminopropyl group also afforded good activity. Of these, all but compound **30** gave IC_{50} values of ≤10 μM in three or more cell lines, with complexes **29** and **30** giving these values in six and five lines, respectively, with cell line overlap in four of these cases (HepG2, Hek293T, MCF7 and 3T3). The differential activity of **32** and **33** is remarkable. In the former, low overall activity is noted while in the latter, with its slightly longer chain, rather significant activity was realised. Together with the similar observation concerning **29** and **30** (both showed good activity but the benzyl group with its additional chain length was better), this aspect may lead to improved activity in future studies if the chain length is manipulated.

The MTT assay measures cell viability as a function of the cell's metabolic activity. However, there are several forms of cell death that can lead to loss of cell viability. Apoptosis is one of these forms of cell death. One of the hallmarks of cancer cells is that these cells are resistant to this form of cell death [61]. Apoptosis is therefore a therapeutic target for the development of anticancer drugs [62] and compounds with

Table 3
Summary of the cytotoxic IC_{50} values (μM) after treatment with P,N gold(I) complexes.[a]

Compound	KMST6	A549J	Caski	HepG2	HeLa	HT29	H157	Hek293T	Jurkat T	MCF7	MG63	CHO	3T3
20	‡	‡	90	‡	90	90	60	25	‡	50	‡	‡	50
22	38	50	80	30	85	15	30	<10	20	20	25	30	45
23	‡	‡	‡	‡	15	60	98	50	18	48	<10	37	15
24	90	60	‡	20	15	80	28	18	50	20	95	35	80
25	‡	‡	‡	‡	‡	‡	‡	60	80	‡	‡	85	‡
26	48	60	‡	20	12	10	25	<10	<10	15	27	25	15
27	‡	‡	‡	48	34	<10	98	<10	25	98	20	65	<10
28	‡	‡	98	48	35	35	96	26	25	30	40	74	25
29	37	63	50	10	<10	20	28	<10	<10	10	12	18	<10
30	‡	20	75	10	‡	10	45	10	45	10	20	60	<10
31	‡	‡	‡	48	35	50	‡	10	<10	48	25	70	18
32	‡	‡	80	‡	‡	90	50	50	20	90	30	‡	50
33	30	30	68	10	12	12	28	<10	50	10	180	25	<10
34	‡	‡	70	25	22	50	30	10	<10	‡	<10	90	18
35	30	30	85	<10	16	45	25	28	28	10	<10	27	45

[a] ‡ indicates an IC_{50} of more than 100 μM; values reported are the average of at least triplicate experiments and standard deviations did not exceed 5%. The IC_{50} values for the positive control, cisplatin, were more than 100 μM for all the cell lines tested in this study.

pro-apoptotic activity are potential leads for the development of anticancer drugs. Hence, we also investigated whether the free ligands and the gold(I) complexes can induce apoptosis in the cell lines used in this study. The cells were treated for 24 h with 50 μM of the compounds and apoptosis was quantified by flow cytometry using the APOP*ercentage*™ assay (Tables 4 and 5). For the purpose of this study, treatments that caused apoptosis in more than 50% of the cells were considered to be significant. Compared to the other ligands, **7** demonstrated the highest pro-apoptotic activity (Table 4). Ligand **7** induced significant levels of apoptosis in five of the cell lines screened in this study, while most of the other ligands induced significant levels of apoptosis in only one cell line. Ligands **16**, **17** and **18** did not induce significant levels of apoptosis in any of the cell lines screened in this study. Compared to the other cell lines, Jurkat T cells were more susceptible to the pro-apoptotic effects of the ligands. Eleven of the ligands induced significant levels of apoptosis in Jurkat T cells. None of the ligands was able to induce significant levels of apoptosis in six of the cell lines (Caski, HeLa, HT29, MG-63, Hek293T and NIH 3T3) screened in this study. Amongst the gold(I) complexes, **29** demonstrated the highest pro-apoptotic activity inducing significant levels of apoptosis in all thirteen cell lines screened in this study (Table 5). Complex **35** demonstrated the lowest pro-apoptotic activity, inducing significant levels of apoptosis in only one cell line, Jurkat T. Complexes **20**, **22**, **31**, **32**, and **34** induced significant levels of apoptosis in between 7 and 10 of the cell lines, respectively. Jurkat T cells were more sensitive to the pro-apoptotic activity of the gold(I) complexes. All fifteen gold(I) complexes induced significant levels of apoptosis in these cells. The non-cancerous cell line, KMST6 was the most resistant cell line with only one of the gold(I) complexes, **29** inducing significant levels of apoptosis in KMST6 cells. With 10 and 9 of the gold(I) complexes inducing significant levels of apoptosis in CHO and HeLa cells, respectively, these two cell lines were also very susceptible to the pro-apoptotic activity of the gold(I) complexes. Interestingly, while both the MTT assay and the APOP*ercentage*™ assay showed that **22** and **29** are the most cytotoxic compounds, it is only the APOP*ercentage*™ assay that shows that **7**, **20**, **31**, **32** and **34** are cytotoxic. In addition, while the MTT assay showed that **35** is one of the most cytotoxic compounds, the APOP*ercentage*™ assay showed that **35** is one of the least cytotoxic compounds. This apparent contradiction can be explained by the fact that the two assays use very different test principles. The MTT assay is an enzyme dependent assay and although this assay is routinely used to assess toxicity, it is known that test compounds that inhibit enzyme activity can affect the MTT assay [63].

As with the MTT assay, the ligands showed low overall cytotoxicity and their data were therefore not interpreted for a structure activity point of view. In the gold complexes, good cytotoxicity was noted for several imine and amine compounds, as opposed to the MTT assay where principal activity was found in the amines. Nevertheless, the amine complexes were more active than the imines. Within the imines (**20**–**28**), greatest activity tended to be found in non-polar substituents with lower steric hindrance (compounds **20** and **22**), but **25** (R = 2-pyridylethyl), **26** (R = 3-dimethylaminopropyl) and **27** (R = 2-thiophenylethyl) induced >95% apoptosis in two cell lines. In all cases, CHO and Jurkat cell lines were susceptible. In the amine complexes, greatest cytotoxicity was achieved with **29** (R = benzyl), **30** (R = phenyl), **31** (R = isopropyl), **32** (R = 2-pyridylethyl) and **34** (R = 3-dimethylaminopropyl). When using a low hurdle (≥50% apoptosis), there is little to learn about structure activity relationships. With a higher bar (≥90% apoptosis), it becomes evident that **29**, **30**, **31** and **34** presented the highest levels of cytotoxicity. In all cases, Jurkat cells were found to be susceptible. Across all cell lines and all complexes tested, CHO and Jurkat cells were most susceptible. Of all of the compounds tested, **29** is the most promising and would be a good candidate for additional structural manipulations.

Based on the cytotoxicity results from the MTT and apoptosis assays, the most promising ligand and gold(I) complex (**7** and **29**, respectively) were submitted to the 60-cell line screen of the NIH DTP [64]. Results of the initial one-dose screen highlighted a 17.3% mean growth inhibition for iminophosphine ligand **7** at a one-dose concentration of 10 μM (range of 61.12 and delta value of 35.77), while **29** proved much more potent, with a mean cell lethality of 40.5% at a one-dose concentration of 10 μM (range of 119.78 and delta value of 35.20). While gold(I) complex **29** progressed to the more in-depth five-dose screen, the promising cytotoxic effects could not be reproduced in the dose–response assay. Although neither of the two compounds submitted was found to be sufficiently potent anticancer agents to warrant further screening by the NCI, valuable data could be gathered from the NCI COMPARE program in terms of the proposed mechanism of action of the gold(I)-based test compound **29**. Specifically, a correlation of 0.505 could be found between the cell line fingerprints of test compound **29** and cytembena, a cytostatic agent found in the DTP database, that has been reported to interfere with the synthesis of cellular DNA [65]. Furthermore, a 0.356 correlation could be found between **29** and L-buthionine sulfoximine, another compound from the DTP database, reported to inhibit glutathione synthase and the formation of glutathione from *gamma*-glutamylcysteine, resulting in a depletion of cellular glutathione and leading to cell death (apoptosis) due to the unrestricted formation of reactive oxygen species (ROS) [66]. It is thus conceivable

Table 4
Levels of apoptosis (% apoptosis) as determined by the APOP*ercentage*™ technique after treatment with the P,N ligands.[a]

Phosphine ligand	A549J	Caski	CH0	HepG2	HeLa	HT29	H157	Jurkat	KMST6	MCF7	MG-63	Hek	3T3
5	44 ± 1	44 ± 2	12 ± 3	24 ± 2	43 ± 2	22 ± 1	48 ± 3	68 ± 8	22 ± 2	42 ± 1	22 ± 3	44 ± 3	43 ± 3
6	32 ± 1	45 ± 1	13 ± 2	13 ± 2	27 ± 2	24 ± 2	45 ± 1	99 ± 1	30 ± 4	48 ± 2	15 ± 1	38 ± 4	15 ± 4
7	57 ± 3	36 ± 1	88 ± 1	50 ± 1	30 ± 2	27 ± 4	48 ± 4	98 ± 1	50 ± 5	10 ± 2	20 ± 2	22 ± 2	22 ± 2
8	20 ± 1	44 ± 3	18 ± 1	25 ± 3	22 ± 3	18 ± 3	22 ± 2	98 ± 1	23 ± 2	12 ± 3	28 ± 2	48 ± 3	35 ± 3
9	17 ± 2	40 ± 5	28 ± 1	36 ± 2	40 ± 3	29 ± 1	37 ± 2	98 ± 1	21 ± 1	22 ± 2	11 ± 3	66 ± 1	28 ± 2
10	41 ± 3	32 ± 2	16 ± 2	28 ± 1	38 ± 2	28 ± 3	44 ± 2	98 ± 1	20 ± 3	63 ± 6	19 ± 1	50 ± 2	32 ± 1
11	22 ± 1	38 ± 2	18 ± 1	20 ± 4	49 ± 4	33 ± 4	32 ± 1	98 ± 1	19 ± 1	10 ± 3	11 ± 1	44 ± 3	27 ± 2
12	27 ± 3	46 ± 4	13 ± 1	18 ± 2	40 ± 3	36 ± 2	38 ± 3	84 ± 1	26 ± 2	60 ± 10	41 ± 2	23 ± 1	29 ± 3
13	31 ± 1	18 ± 3	15 ± 3	22 ± 3	40 ± 2	41 ± 2	36 ± 1	98 ± 1	28 ± 3	49 ± 1	11 ± 3	25 ± 3	35 ± 1
14	39 ± 1	48 ± 2	19 ± 1	38 ± 5	32 ± 4	43 ± 2	30 ± 3	98 ± 1	43 ± 1	8 ± 3	22 ± 2	19 ± 2	41 ± 2
15	22 ± 2	26 ± 4	32 ± 1	24 ± 1	28 ± 2	44 ± 2	22 ± 5	98 ± 1	44 ± 1	5 ± 2	20 ± 1	30 ± 3	33 ± 1
16	34 ± 3	20 ± 2	18 ± 3	15 ± 4	12 ± 2	24 ± 1	14 ± 3	40 ± 1	40 ± 3	25 ± 1	20 ± 3	18 ± 2	28 ± 2
17	38 ± 2	28 ± 2	26 ± 1	36 ± 2	16 ± 1	18 ± 1	24 ± 3	38 ± 1	38 ± 2	32 ± 2	31 ± 4	16 ± 1	32 ± 1
18	22 ± 1	37 ± 3	10 ± 2	28 ± 2	26 ± 3	24 ± 3	72 ± 1	28 ± 1	48 ± 2	17 ± 2	22 ± 2	15 ± 2	36 ± 2
19	20 ± 2	39 ± 3	28 ± 1	33 ± 1	21 ± 1	27 ± 1	40 ± 3	41 ± 1	33 ± 1	40 ± 2	25 ± 3	11 ± 3	34 ± 4

[a] Values reported are the average of at least triplicate experiments.

Table 5
Levels of apoptosis (% apoptosis) as determined by the APO*Percentage*™ technique after treatment with the P,N gold(I) complexes.[a]

Complexes	A549J	Caski	CH0	HepG2	HeLa	HT29	H157	Jurkat	KMST6	MCF7	MG-63	Hek	3T3
20	50 ± 3	54 ± 2	100 ± 1	46 ± 5	43 ± 2	48 ± 2	98 ± 1	99 ± 1	22 ± 2	88 ± 5	92 ± 4	72 ± 4	50 ± 1
22	66 ± 4	45 ± 1	53 ± 2	45 ± 2	77 ± 2	66 ± 3	97 ± 2	98 ± 1	30 ± 4	98 ± 1	75 ± 4	60 ± 6	54 ± 2
23	30 ± 2	36 ± 4	46 ± 1	32 ± 1	77 ± 2	34 ± 1	44 ± 4	98 ± 1	15 ± 3	10 ± 2	20 ± 2	42 ± 2	17 ± 4
24	40 ± 2	44 ± 3	98 ± 1	30 ± 2	62 ± 3	30 ± 1	42 ± 2	98 ± 1	23 ± 2	12 ± 3	28 ± 2	48 ± 3	24 ± 2
25	37 ± 4	40 ± 5	98 ± 1	40 ± 3	40 ± 3	22 ± 3	40 ± 2	98 ± 1	21 ± 1	22 ± 2	11 ± 3	46 ± 1	36 ± 1
26	26 ± 4	32 ± 2	96 ± 2	34 ± 1	58 ± 2	35 ± 2	44 ± 2	98 ± 1	20 ± 3	8 ± 2	19 ± 1	40 ± 2	28 ± 2
27	45 ± 2	38 ± 2	98 ± 1	28 ± 4	49 ± 4	27 ± 2	32 ± 1	98 ± 1	19 ± 1	10 ± 3	11 ± 1	44 ± 3	40 ± 3
28	46 ± 2	46 ± 4	98 ± 1	20 ± 3	40 ± 3	25 ± 4	38 ± 3	88 ± 4	26 ± 2	9 ± 2	41 ± 2	43 ± 1	42 ± 1
29	80 ± 4	88 ± 3	66 ± 3	85 ± 2	80 ± 2	76 ± 5	99 ± 1	99 ± 1	70 ± 5	99 ± 1	91 ± 5	85 ± 5	77 ± 2
30	40 ± 4	48 ± 2	98 ± 1	48 ± 2	72 ± 4	28 ± 4	30 ± 3	98 ± 1	43 ± 1	8 ± 3	22 ± 2	46 ± 2	66 ± 2
31	48 ± 3	66 ± 4	98 ± 1	50 ± 5	68 ± 2	59 ± 2	99 ± 1	98 ± 1	44 ± 1	5 ± 2	20 ± 1	40 ± 3	56 ± 1
32	49 ± 2	60 ± 2	18 ± 3	64 ± 1	62 ± 2	40 ± 2	78 ± 3	80 ± 5	40 ± 3	98 ± 1	60 ± 6	50 ± 4	62 ± 1
33	48 ± 2	48 ± 2	44 ± 1	44 ± 3	36 ± 1	40 ± 1	82 ± 2	98 ± 1	38 ± 2	32 ± 2	31 ± 4	30 ± 1	34 ± 2
34	65 ± 2	40 ± 3	10 ± 2	45 ± 1	56 ± 3	63 ± 3	42 ± 1	98 ± 1	48 ± 2	97 ± 1	88 ± 8	61 ± 4	28 ± 3
35	46 ± 2	48 ± 4	32 ± 4	38 ± 4	42 ± 1	41 ± 2	40 ± 3	98 ± 1	33 ± 1	40 ± 2	25 ± 3	25 ± 3	46 ± 1

[a] Values reported are the average of at least triplicate experiments.

that complex **29** may act on one or both of these pathways. It is interesting to note that the biologically active compounds (ligands and gold-complexes alike) showed potential for selective cytotoxicity in the range of cancerous cell lines tested. The differences observed in selectivity and potency profiles of the free ligands vs the gold(I) complexes, coupled with the variable cytotoxic effect displayed by the biologically active compounds across the panel of cell lines, illustrate the possibility of tailoring the potency of the ligands, either through the inclusion of gold(I) to the ligand systems, or by incorporating variability into the molecular structure through changing the nitrogen-borne substituent of both imino- and aminophosphine analogues (Fig. 8).

3. Conclusions

A range of new P,N ligands has been synthesised that represent the nitrogen in sp^2 and sp^3 hybridisation states. Complexation to Au(I) allowed the formation of several new gold(I) complexes of which representative examples were characterised by single crystal X-ray crystallography. Biological evaluations into the cytotoxicity of the free ligands and gold(I) complexes on a range of cancerous and non-cancerous human and rodent cell lines show that the complexes are more highly cytotoxic than their corresponding ligands towards the cancer cell lines tested, and display lower cytotoxicity towards healthy cells. The enhanced cytotoxicity of the gold(I) complexes as compared to the free ligands was confirmed in the 60 cell-line fingerprint screen of the NIH DTP. Additionally, the high pro-apoptotic activity of **29** as determined in the APO*Percentage* assay was supported by correlations between the characteristic 60 cell-line fingerprint of **29** and that of L-buthionine sulfoximine, a known pro-apoptotic agent. While no conclusive structure–activity relationships could be established for this group of compounds, the differences in activity due to the R-group structure are notable and point towards the value of additional studies in this area, which would include in vitro investigations to elucidate the mechanism by which the observed pro-apoptotic activity is conferred. These studies may prove to add to the currently limited knowledge-base on biologically active gold(I) compounds.

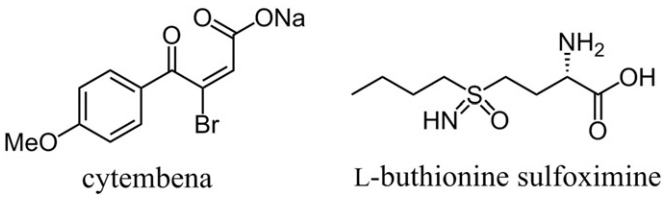

Fig. 8. Molecular structures of cytembena and L-buthionine sulfoximine.

4. Experimental section

4.1. General methods and materials

Chemical ionisation mass spectrometry (CIMS) was performed on a Finnigan-Matt 8200 spectrometer at a 70 eV ionisation potential. Fast atom bombardment mass spectra (FAB-MS) were acquired with a VG70SE mass spectrometer under the control of a MS Services data system, with glycerol matrices. ^{1}H-, ^{13}C- and ^{31}P NMR data were obtained on a Varian Gemini-300 Hz spectrometer. The data are reported as parts per million relative to TMS and referenced to $CDCl_3$. The peak multiplicities are abbreviated as follows: s — singlet; d — doublet; dd — doublet of doublets; t — triplet; tt — triplet of triplets; p — pentet; sx — sextet; and m — multiplet. The coupling constant (J) is calculated in Hertz and reported to the nearest 0.1 Hz [67]. Where appropriate, $J_{C,P}$ values are given as observed in the ^{13}C NMR spectra of the compounds. Infrared spectroscopy (IR) was performed on a Perkin-Elmer 881 spectrometer in $CHCl_3$ solvent or KBr pellets. The characteristic peaks are reported in wavenumber (cm^{-1}). Melting points were collected on a DSC822^e Mettler Toledo differential scanning calorimetry instrument. All solvents used were chemically pure or pre-purified [68,69]. Hexane was purified by distillation. Toluene and diethyl ether were pre-dried over an Al_2O_3 column and then dried over sodium-benzophenone under nitrogen until the dark blue colour of the benzophenone ketyl persisted. Solvents were removed by rotary evaporation under reduced pressure and purification performed by bulb-to-bulb vacuum distillation using Kugel–Rohr distillation apparatus. All other reagents were analytically and synthetically pure. All reagents and starting materials were degassed before use to minimise the oxidation of the iminophosphine products. All experiments were performed in oven-dried, flamed out flasks under an atmosphere of UHP argon. A Dean–Stark apparatus was used in all cases for the azeotropic removal of water.

4.2. General procedure for the synthesis of iminophosphine ligands (**4**–**12**). Procedure A

The iminophosphine ligands were prepared according to the method reported by Shirakawa and co-workers [70]. To 2-(diphenylphosphino)benzaldehyde (**1**) (200 mg, 0.689 mmol) 0.758 mmol (1.1 M equivalent) of the corresponding amine and 10 mL of freshly distilled toluene were added. The mixture was stirred under reflux (150–160 °C oil bath temperature) for 6 h. The solvent was removed in vacuo and the crude product was purified by bulb-to-bulb vacuum distillation (170 °C at 0.05 mm Hg, consistently used for all products) using a Kugel Rohr apparatus into which argon was continuously piped to prevent the ingress

of oxygen. Since the iminophosphine products were unstable on silica, no R_f-values are included for the iminophosphine ligands.

4.2.1. (Z)-N-(2-(Diphenylphosphino)benzylidene)-methanamine (**4**)

Methylamine (0.758 mmol, 0.712 mL) was added to the 2-(diphenylphosphino) benzaldehyde mixture and treated according to general procedure A to provide **4** as white powder after distillation (0.659 mmol, 0.200 g, 87%). Colourless single crystals were grown from a layered solution of chloroform and *n*-hexane. mp: 117.5–119.0 °C; ^{1}H NMR: (300 MHz, $CDCl_3$) δ_H 8.93 (dq, J = 4.5 and 1.5 Hz, 1H), 7.98 (ddd, J = 7.7, 4.1 and 1.4 Hz, 1H), 7.40–7.24 (m, 12H), 6.89 (ddd, J = 7.6, 4.7 and 1.3 Hz, 1H), and 3.38 (d, J = 1.5 Hz, 3H); ^{13}C NMR: (75 MHz, $CDCl_3$) δ_C 160.8 (d, J = 22.4 Hz), 139.5 (d, J = 17.4 Hz), 137.0 (d, J = 19.1 Hz), 136.3 (d, J = 9.7 Hz), 133.8 (d, J = 19.7 Hz), 133.3 (d, J = 10.8 Hz), 130.1, 128.9, 128.7, 128.5 (d, J = 7.1 Hz), 127.0 (d, J = 14.3 Hz), and 47.9 (d, J = 11.7 Hz); ^{31}P NMR: (121 MHz, $CDCl_3$) δ_P −14.1; IR: ν_{max} ($CHCl_3$)/cm^{-1} 2879 and 1641; HRMS calcd for $C_{20}H_{19}NP$ ([M + H]$^+$): m/z 304.1255; found: 304.1253. Crystal data are available in the Supplementary Information.

4.2.2. N-(2-(Diphenylphosphino)phenyl)-methylene-butylamine (**5**)

n-Butylamine (0.758 mmol, 0.078 mL) was added to the 2-(diphenylphosphino) benzaldehyde mixture and treated according to general procedure A to provide **5** as a viscous orange oil after distillation (0.668 mmol, 0.231 g, 97%). ^{1}H NMR: (300 MHz, $CDCl_3$) δ_H 8.71 (d, J = 4.2 Hz, 1H), 7.88 (dd, J = 3.9 Hz, 1H), 7.30–7.14 (m, 12H), 6.77 (dd, J = 7.7 and 4.7 Hz, 1H), 3.38 (t, J = 6.8 Hz, 2H), 1.37 (p, J = 7.1 Hz, 2H), 1.02 (sx, J = 7.4 Hz, 2H), and 0.71 (t, J = 7.2 Hz, 3H); ^{13}C NMR: (75 MHz, $CDCl_3$) δ_C 159.3 (d, J = 21.5 Hz), 139.6 (d, J = 16.9 Hz), 137.1 (d, J = 18.9 Hz), 136.4 (d, J = 9.5 Hz), 134.0 (d, J = 19.7 Hz), 133.1, 130.0, 128.8, 128.7, 128.5 (d, J = 7.2 Hz), 127.5 (d, J = 4.4 Hz), 61.2, 32.6, 20.1, and 13.8; ^{31}P NMR: (121 MHz, $CDCl_3$) δ_P −13.3; IR: ν_{max} ($CHCl_3$)/cm^{-1} 2964 and 1647; CIMS: m/z 345 ([M]$^+$, 86%) and 288 ([M − C_4H_9]$^+$, 100%).

4.2.3. N-(2-(Diphenylphosphino)phenyl)-methylene benzylamine (**6**)

Benzylamine (0.758 mmol, 0.082 mL) was added to the 2-(diphenylphosphino) benzaldehyde mixture and treated according to general procedure A to provide **6** as a viscous yellow oil after distillation that was precipitated as a white powder from methanol (0.661 mmol, 0.251 g, 96%). mp: 105–106.5 °C; ^{1}H NMR: (300 MHz, $CDCl_3$) δ_H 8.94 (d, J = 5.4 Hz, 1H), 7.97 (dd, J = 7.4 and 3.8 Hz, 1H), 7.32–7.08 (m, 15H), 6.97–6.94 (m, 2H), 6.80 (dd, J = 6.8 and 5.3 Hz, 1H), and 4.59 (s, 2H); ^{13}C NMR: (75 MHz, $CDCl_3$) δ_C 160.5 (d, J = 22.3 Hz), 139.3 (d, J = 17.2 Hz), 138.9, 137.5 (d, J = 18.9 Hz), 136.3 (d, J = 9.5 Hz), 134.0 (d, J = 20.0 Hz), 133.2, 130.4, 128.9, 128.6 (d, J = 7.1 Hz), 128.3, 128.0, 127.6 (d, J = 4.1 Hz), 126.7, and 65.1; ^{31}P NMR: (121 MHz, $CDCl_3$) δP −13.6; IR: νmax ($CHCl_3$)/cm^{-1} 2845 and 1640; CIMS: m/z 379 ([M]$^+$, 12%) and 288 ([M − C_7H_7]$^+$, 100%).

4.2.4. N-(2-(Diphenylphosphino)phenyl)-methylene benzenamine (**7**)

Aniline (0.758 mmol, 0.069 mL) was added to the 2-(diphenylphosphino) benzaldehyde mixture and treated according to general procedure A to provide **7** as a viscous light yellow oil after distillation (0.668 mmol, 0.244 g, 97%). ^{1}H NMR: (300 MHz, $CDCl_3$) δ_H 8.98 (d, J = 5.4 Hz), 8.12 (dd, J = 7.1 and 3.8 Hz, 1H), 7.36 (t, J = 7.6 Hz, 1H), 7.27–7.14 (m, 14H), 7.09–7.04(m, 1H), and 6.87–6.81 (m, 2H); ^{13}C NMR: (75 MHz, $CDCl_3$) δ_C 158.8 (d, J = 21.8 Hz), 151.6, 139.1 (d, J = 16.4 Hz), 138.6 (d, J = 20.0 Hz), 136.4 (d, J = 9.5 Hz), 134.0 (d, J = 19.8 Hz), 133.5, 130.8, 128.9 (d, J = 2.9 Hz), 128.7 (d, J = 7.1 Hz), 128.1 (d, J = 4.1 Hz), 125.9, and 120.9; ^{31}P NMR: (121 MHz, $CDCl_3$) δ_P −12.9; IR: ν_{max} ($CHCl_3$)/cm^{-1} 3019 and 1626; CIMS: m/z 365 ([M]$^+$, 89%) and 288 ([M − C_6H_5]$^+$, 100%).

4.2.5. (2-Diphenylphosphanyl-benzylidene)-isopropyl amine (**8**)

Isopropylamine (0.758 mmol, 0.065 mL) was added to the 2-(diphenylphosphino) benzaldehyde mixture and treated according to general procedure A to provide **8** as a viscous light yellow oil after distillation (0.668 mmol, 0.221 g, 97%). ^{1}H NMR: (300 MHz, $CDCl_3$) δ_H 8.71 (d, J = 4.5 Hz, 1H), 7.81 (dd, J = 7.4 and 3.8 Hz, 1H), 7.23–7.07 (m, 12H), 6.64 (dd, J = 7.5 and 4.8 Hz, 1H), 3.23 (sp, J = 6.3 Hz, 1H), and 0.89 (d, J = 3.2 Hz, 6H); ^{13}C NMR: (75 MHz, $CDCl_3$) δ_C 156.9 (d, J = 20.9 Hz), 139.6 (d, J = 16.9 Hz), 137.0 (d, J = 18.6 Hz), 136.4 (d, J = 9.5 Hz), 134.0 (d, J = 20.0 Hz), 132.9, 129.9, 128.8, 128.7, 128.5 (d, J = 7.2 Hz), 127.4 (d, J = 4.0 Hz), 61.2, and 23.9; ^{31}P NMR: (121 MHz, $CDCl_3$) δ_P −13.0; IR: ν_{max} ($CHCl_3$)/cm^{-1} 2940 and 1642; CIMS: m/z 332 ([M]$^+$, 100%), 288 ([M − C_3H_7]$^+$, 82%).

4.2.6. (2-Diphenylphosphanyl-benzyl)-(2-pyrid-2-yl-ethyl)-amine (**9**)

2-(Aminoethyl)pyridine (0.758 mmol, 0.091 mL) was added to the 2-(diphenylphosphino) benzaldehyde mixture and treated according to general procedure A to provide **9** as a viscous yellow oil after distillation (0.634 mmol, 0.250 g, 92%). ^{1}H NMR: (300 MHz, $CDCl_3$) δ_H 8.76 (d, J = 4.5 Hz), 8.37 (d, J = 4.2 Hz, 1H), 7.84 (dd, J = 7.2 and 3.3 Hz, 1H), 7.36 (td, J = 7.7 and 1.7 Hz, 1H), 7.28–7.13 (m, 12H), 6.93 (d, J = 7.2 Hz, 2H), 6.77 (dd, J = 7.2 and 5.1 Hz, 1H), 3.79 (t, J = 7.2 Hz, 2H), and 2.88 (t, J = 7.2 Hz, 2H); ^{13}C NMR: (75 MHz, $CDCl_3$) δ_C 160.1 (d, J = 20.9 Hz), 159.7, 149.1, 139.4 (d, J = 17.2 Hz), 137.2 (d, J = 19.4 Hz), 136.5 (d, J = 9.8 Hz), 135.9, 133.8 (d, J = 19.7 Hz), 133.3, 130.0, 128.7, 128.6, 128.4 (d, J = 7.2 Hz), 127.5 (d, J = 4.3 Hz), 123.3, 121.0, 60.7, and 39.4; ^{31}P NMR: (121 MHz, $CDCl_3$) δ_P −13.5; IR: ν_{max} ($CHCl_3$)/cm^{-1} 2963 and 1657; CIMS: m/z 395 ([M]$^+$, 100%) and 288 ([M − $C_7H_8N_2$]$^+$, 62%).

4.2.7. N′-(2-Diphenylphosphanyl-benzylidene)-N,N-dimethyl-propane-1,3-diamine (**10**)

3-Dimethylamino-propyl amine (0.758 mmol, 0.095 mL) was added to the 2-(diphenylphosphino) benzaldehyde mixture and treated according to general procedure A to provide **10** as a viscous yellow oil after distillation (0.634 mmol, 0.237 g, 92%). ^{1}H NMR: (300 MHz, $CDCl_3$) δ_H 8.78 (d, J = 4.5 Hz, 1H), 7.87 (dd, J = 7.1 and 3.5 Hz, 1H), 7.28–7.14 (m, 12H), 6.76 (dd, J = 6.9 and 5.1 Hz, 1H), 3.40 (t, J = 6.8 Hz, 2H), 2.08–1.97 (m, 8H), and 1.56 (p, J = 7.1 Hz, 2H); ^{13}C NMR: (75 MHz, $CDCl_3$) δ_C 159.4 (d, J = 20.9 Hz), 139.4 (d, J = 17.2 Hz), 137.0 (d, J = 20.9 Hz), 136.4 (d, J = 9.8 Hz), 133.8 (d, J = 20.0 Hz), 133.1, 129.9, 128.7, 128.6, 128.4 (d, J = 7.1 Hz), 127.5 (d, J = 4.4 Hz), 59.3, 57.3, 45.3, and 28.6; ^{31}P NMR: (121 MHz, $CDCl_3$) δ_P −13.1; IR: ν_{max} ($CHCl_3$)/cm^{-1} 2949 and 1643; CIMS: m/z 375 ([M]$^+$, 100%) and 303 ([M − $C_5H_{12}N$]$^+$, 20%).

4.2.8. (2-Diphenylphosphanyl-benzylidene)-(2-thiophen-2-yl-ethyl)-amine (**11**)

2-Thiophenethylamine (0.758 mmol, 0.088 mL) was added to the 2-(diphenylphosphino) benzaldehyde mixture and treated according to general procedure A to provide **11** as a viscous rich-yellow oil after distillation (0.648 mmol, 0.259 g, 94%). ^{1}H NMR: (300 MHz, $CDCl_3$) δ_H 8.78 (d, J = 4.8 Hz), 7.90 (dd, J = 7.5 and 3.6 Hz, 1H), 7.33–7.15 (m, 12H), 6.97 (d, J = 5.4 Hz, 1H), 6.82–6.75 (m, 2H), 6.65 (d, J = 3.3 Hz, 1H), 3.66 (t, J = 7.4 Hz, 2H), and 2.90 (t, J = 7.4 Hz, 2H); ^{13}C NMR: (75 MHz, $CDCl_3$) δ_C 160.4 (d, J = 21.2 Hz), 142.3, 139.4 (d, J = 17.2 Hz), 137.4 (d, J = 19.2 Hz), 136.5 (d, J = 9.5 Hz), 133.9 (d, J = 20.0 Hz), 133.4, 130.2, 128.9, 128.8, 128.6 (d, J = 7.1 Hz), 127.7 (d, J = 4.3 Hz), 126.6, 124.8, 123.4, 62.5, and 31.3; ^{31}P NMR: (121 MHz, $CDCl_3$) δ_P −13.4; IR: ν_{max} ($CHCl_3$)/cm^{-1} 3051, 3026, 2939, 2837, and 1635; CIMS: m/z 400 ([M]$^+$, 100%) and 288 ([M − C_6H_7S] $^+$, 22%).

4.2.9. tert-Butyl-(2-diphenylphosphanyl-benzylidene)-amine (**12**)

tert-Butylamine (0.758 mmol, 0.079 mL) was added to the 2-(diphenylphosphino) benzaldehyde mixture and treated according to general procedure A to provide **12** as a creamy white solid after

distillation (0.661 mmol, 0.228 g, 96%). Colourless, needle-like single crystals were grown from ethanol. mp: 115–116.5 °C; ^{1}H NMR: (300 MHz, $CDCl_3$) δ_H 8.67 (d, J = 5.1 Hz, 1H), 7.82 (dd, J = 7.1 and 3.5 Hz, 1H), 7.28–7.10 (m, 12H), 6.72 (dd, J = 6.8 and 5.3 Hz, 1H), and 0.95 (s, 9H); ^{13}C NMR: (75 MHz, $CDCl_3$) δ_C 154.3 (d, J = 20.3 Hz), 139.9 (d, J = 15.8 Hz), 137.3 (d, J = 18.3 Hz), 136,5 (d, J = 9.5 Hz), 134.1 (d, J = 20.0 Hz), 132.7, 129.6, 128.7, 128.5 (d, J = 7.1 Hz), 127.3 (d, J = 3.7 Hz), 57.6, and 29.4; ^{31}P NMR: (121 MHz, $CDCl_3$) δ_P −11.6; IR: ν_{max} ($CHCl_3$)/cm^{-1} 2961 and 1638; CIMS: m/z 346 ([M]$^+$, 26%) and 288 ([M − C_4H_9]$^+$, 100%).

4.3. General procedure for the preparation of aminophosphine ligands (**13**–**19**). Procedure B

To 2-(diphenylphosphino)-benzaldehyde (200 mg, 0.689 mmol) 0.758 mmol (1.1 M equivalents) of the corresponding amine and 10 mL of freshly distilled toluene were added. The mixture was stirred under reflux for 6 h. The toluene was removed in vacuo and anhydrous MeOH and 3 equivalents $NaBH_4$ were added to the residue under argon flow. The reactions were left to stir at room temperature for 12 h, quenched with distilled water and extracted with CH_2Cl_2 (×3). The organic phase was dried over anhydrous Na_2SO_4. The aminophosphine ligands were obtained in pure form following bulb-to-bulb vacuum distillation (170 °C, 0.05 mm Hg).

4.3.1. N-(2-Diphenylphosphinobenzyl)benzylamine (**13**)

Benzylamine (0.758 mmol, 0.082 mL) was used as the amine starting material to prepare iminophosphine intermediate **6**, and immediately reduced as per the general aminophosphine synthesis (Procedure B) above. The pure aminophosphine product **13** was obtained as a light yellow oil after distillation (0.537 mmol, 0.205 g, 78%). ^{1}H NMR: (300 MHz, $CDCl_3$) δ_H 7.55 (dd, J = 7.2 and 4.2, 1H), 7.41–7.19 (m, 17H), 6.98 (dd, J = 7.4 and 4.7 Hz, 1H), 4.09 (s, 2H), 3.73 (d, J = 2.7 Hz, 2H), and 1.69 (s, 1H); ^{13}C NMR: (75 MHz, $CDCl_3$) δ_C 144.4 (d, J = 23.6 Hz), 140.2, 136.6 (d, J = 9.5 Hz), 135.7 (d, J = 13.5 Hz), 133.8 (d, J = 19.6 Hz), 133.6, 129.2 (d, J = 5.5 Hz), 128.9, 128.6, 128.5 (d, J = 7.1 Hz), 128.1, 128.0, 127.2, 126.6, 53.2, and 52.0 (d, J = 20.6 Hz); ^{31}P NMR: (121 MHz, $CDCl_3$) δ_P −15.6; IR: ν_{max} ($CHCl_3$)/cm^{-1} 3026 and 1438; CIMS: m/z 381 ([M]$^+$, 41%) and 275 ([M − C_7H_8N]$^+$, 83%).

4.3.2. N-(2-Diphenylphosphinobenzyl)phenylamine (**14**)

Aniline (0.758 mmol, 0.069 mL) was used as the amine starting material to prepare iminophosphine intermediate **7**, and immediately reduced as per the general aminophosphine synthesis (Procedure B) above. The pure aminophosphine product **14** was obtained as a fine white powder after distillation (0.558 mmol, 0.205 g, 81%). Colourless single crystals were grown from a layered solution of chloroform and *n*-hexane. mp: 143–145 °C; ^{1}H NMR: (300 MHz, $CDCl_3$) δ_H 7.39–7.37 (m, 1H), 7.26–7.14 (m, 11H), 7.08 (t, J = 7.4 Hz, 1H), 6.99 (t, J = 7.5 Hz, 2H), 6.83 (t, J = 5.4 Hz, 1H), 6.56 (t, J = 6.9 Hz, 1H), 6.30 (d, J = 8.1 Hz, 2H), 4.40 (s, 2H), and 3.82 (br s); ^{13}C NMR: (75 MHz, $CDCl_3$) δ_C 147.6, 143.2 (d, J = 23.2 Hz), 136.2 (d, J = 9.7 Hz), 135.6 (d, J = 14.6 Hz), 133.9 (d, J = 19.7 Hz), 133.5, 129.0, 128.8, 128.6 (d, J = 7.1 Hz), 128.1 (d, J = 5.2 Hz), 127.4, 117.3, 112.8, and 47.0 (d, J = 23.5 Hz); ^{31}P NMR: (121 MHz, $CDCl_3$) δ_P −15.5; IR: ν_{max} ($CHCl_3$)/cm^{-1} 3026 and 1219; CIMS: m/z 367 ([M]$^+$, 24%) and 275 ([M − C_6H_6N]$^+$, 100%). Crystal data are available in the Supplementary Information.

4.3.3. (2-Diphenylphosphanyl-benzyl)-isopropyl amine (**15**)

Isopropyl amine (0.758 mmol, 0.065 mL) was used as the amine starting material to prepare iminophosphine intermediate **8**, and immediately reduced as per the general aminophosphine synthesis (Procedure B) above. The pure aminophosphine product **15** was obtained as a semi-translucent viscous white oil after distillation (0.544 mmol, 0.181 g, 79%). ^{1}H NMR: (300 MHz, $CDCl_3$) δ_H 7.44 (ddd, J = 7.3, 4.5 and 1.2 Hz, 1H), 7.30–7.22 (m, 11H), 7.09 (td, J = 7.5 and 1.4 Hz, 1H), 6.88 (ddd, J = 7.6, 3.8 and 1.4 Hz, 1H), 3.87 (s, 2H), 2.56 (sp, J = 6.6 Hz, 1H), and 0.79 (d, J = 6.6 Hz, 6H); ^{13}C NMR: (75 MHz, $CDCl_3$) δ_C 144.4 (d, J = 23.6 Hz), 136.5 (d, J = 9.9 Hz), 135.4 (d, J = 13.7 Hz), 133.6 (d, J = 19.5 Hz), 133.3, 129.1 (d, J = 5.5 Hz), 128.7, 128.4, 128.3 (d, J = 6.8 Hz), 126.9, 49.9 (d, J = 20.6 Hz), 47.7, and 22.5; ^{31}P NMR: (121 MHz, $CDCl_3$) δ_P −15.7; IR: ν_{max} ($CHCl_3$)/cm^{-1} 2945 and 1438; CIMS: m/z 334 ([M]$^+$, 100%).

4.3.4. (2-Diphenylphosphanyl-benzyl)-pyrid-2-ylmethyl amine (**16**)

2-(Aminomethyl)-pyridine (0.758 mmol, 0.078 mL) was used as the amine starting material and the iminophosphine intermediate prepared as per procedure A above. Immediate reduction as per the general aminophosphine synthesis (Procedure B) above, afforded the pure aminophosphine product **16** as a creamy white oil after distillation (0.400 mmol, 0.153 g, 58%). ^{1}H NMR: (300 MHz, $CDCl_3$) δ_H 8.48 (d, J = 4.5 Hz, 1H), 7.52 (d, J = 6.0 Hz, 3H), 7.34–7.06 (m, 14H), 6.89 (t, J = 6.0 Hz, 1H), 4.05 (s, 2H), and 3.82 (s, 2H); ^{13}C NMR: (75 MHz, $CDCl_3$) δ_C 159.7, 149.0, 144.2 (d, J = 24.1 Hz), 136.7 (d, J = 9.8 Hz), 136.2, 135.7 (d, J = 13.7 Hz), 133.8 (d, J = 19.5 Hz), 133.6, 129,0 (d, J = 5.5 Hz), 128.9, 128.6, 128.4 (d, J = 7.1 Hz), 127.2, 121.9, 121.6, 54.5, and 51.9 (d, J = 20.9 Hz); ^{31}P NMR: (121 MHz, $CDCl_3$) δ_P −15.5; IR: ν_{max} ($CHCl_3$)/cm^{-1} 2992 and 1431; CIMS: m/z 383 ([M]$^+$, 30%) and 290 ([M − C_6H_6N]$^+$, 20%).

4.3.5. (2-Diphenylphosphanyl-benzyl)-2-(pyrid-2-yl)-ethyl amine (**17**)

2-(Aminoethyl)pyridine (0.758 mmol, 0.091 mL) was used as the amine starting material to prepare iminophosphine intermediate **9**, and immediately reduced as per the general aminophosphine synthesis (Procedure B) above. The pure aminophosphine product **17** was obtained as a creamy white oil after distillation (0.489 mmol, 0.194 g, 71%). ^{1}H NMR: (300 MHz, $CDCl_3$) δ_H 8.40 (d, J = 4.8 Hz, 1H), 7.43 (td, J = 7.7 and 1.9 Hz, 1H), 7.35 (dd, J = 7.1 and 4.7 Hz, 1H), 7.24–7.12 (m, 12H), 7.04 (td, J = 7.5 and 1.2 Hz, 1H), 6.96 (dd, J = 7.5 and 0.9 Hz, 1H), 6.78 (dd, J = 6.5 and 4.7, 1H), 3.91 (s, 2H), 2.82 (t, J = 6.6 Hz, 2H), 2.71 (t, J = 6.6 Hz, 2H), and 1.42 (s, 1H); ^{13}C NMR: (75 MHz, $CDCl_3$) δ_C 160.2, 149.2, 144.5 (d, J = 23.6 Hz), 136.7 (d, J = 10.2 Hz), 136.1, 135.6 (d, J = 14.0 Hz), 133.7 (d, J = 19.7 Hz), 133.5, 128.9 (d, J = 4.3 Hz), 128.5, 128.5 (d, J = 14.8 Hz), 127.1, 123.1, 121.0, 52.2 (d, J = 20.6 Hz), 48.7, and 38.5; ^{31}P NMR: (121 MHz, $CDCl_3$) δ_P −15.7; IR: ν_{max} ($CHCl_3$)/cm^{-1} 3026 and 1438; CIMS: m/z 397 ([M]$^+$, 100%) and 318 ([M − C_5H_4N]$^+$, 20%).

4.3.6. N′-(2-Diphenylphosphanyl-benzyl)-N,N-dimethyl-propane-1,3-diamine (**18**)

3-Dimethylamino-1-propylamine (0.758 mmol, 0.095 mL) was used as the amine starting material to prepare iminophosphine intermediate **10**, and immediately reduced as per the general aminophosphine synthesis (Procedure B) above. The pure aminophosphine product **18** was obtained as a creamy white oil after distillation (0.475 mmol, 0.179 g, 69%). ^{1}H NMR: (300 MHz, $CDCl_3$) δ_H 7.33 (dd, J = 4.8 and 6.9 Hz, 1H), 7.16–7.13 (m, 11H), 7.99 (t, J = 7.4 Hz, 1H), 6.76 (dd, J = 7.2 and 4.5 Hz, 1H), 3.85 (s, 2H), 2.40 (t, J = 7.1 Hz, 2H), 2.03 (m, 8H), 1.41 (s, 1H), and 1.34 (p, J = 7.2 Hz, 2H); ^{13}C NMR: (75 MHz, $CDCl_3$) δ_C 144.4 (d, J = 23.8 Hz), 136.5 (d, J = 10.3 Hz), 135.4 (d, J = 13.5 Hz), 133.6 (d, J = 19.4 Hz), 133.4, 128.9 (d, J = 5.2 Hz), 128.7, 128.5, 128.3 (d, J = 6.9 Hz), 126.9, 57.7, 52.4 (d, J = 20.6 Hz), 47.5, 45.3, and 27.8; ^{31}P NMR: (121 MHz, $CDCl_3$) δ_P −15.7; IR: ν_{max} ($CHCl_3$)/cm^{-1} 2956, 2831, and 1438; CIMS: m/z 377 ([M]$^+$, 100%) and 298 ([M − $C_5H_{13}N_2$]$^+$, 30%).

4.3.7. N-(2-Diphenylphosphino)benzyl-2-(thiophen-2-yl)ethanamine (**19**)

2-Thiophenethylamine (0.758 mmol, 0.088 mL) was used as the amine starting material to prepare iminophosphine intermediate **11**, and immediately reduced as per the general aminophosphine synthesis

(Procedure B) above. The pure aminophosphine product **19** was obtained as a viscous light yellow oil after distillation (0.537 mmol, 0.216 g, 78%). ^{1}H NMR: (300 MHz, $CDCl_3$) δ_H 7.34 (dd, J = 7.5 and 4.2 Hz, 1H), 7.20–7.14 (m, 11H), 7.03 (t, J = 7.5 Hz, 1H), 6.96 (d, J = 4.8 Hz, 1H), 6.80–6.75 (m, 2H), 6.62 (d, J = 3.0 Hz, 1H), 3.91 (s, 2H), 2.68 (s, 4H), and 1.51 (s, 1H); ^{13}C NMR: (75 Hz, $CDCl_3$) δ_C 144.2 (d, J = 23.5 Hz), 142.5, 136.6 (d, J = 10.0 Hz), 135.6 (d, J = 13.7 Hz), 133.7 (d, J = 19.7 Hz), 133.6, 128.9 (d, J = 5.5 Hz), 128.8, 128.6, 128.4 (d, J = 7.2 Hz), 127.1, 126.6, 124.7, 123.2, 52.1 (d, J = 20.6 Hz), 50.3, and 30.2; ^{31}P NMR: (121 MHz, $CDCl_3$) δ_P −15.7; IR: ν_{max} ($CHCl_3$)/cm^{-1} 3053, 3031, 3003, 2916, and 2825; CIMS: m/z 402 ($[M]^+$, 100%) and 304 ($[M-C_5H_5S]^+$, 85%).

4.4. General procedure for the preparation of iminophosphine gold(I) complexes (**20**–**28**). Procedure C

[AuCl(THT)] (THT = tetrahydrothiophene) was prepared according to literature methods [71]. To a stirred solution of the iminophosphine ligand (0.150 mmol) in 5 mL diethyl ether, 1 equivalent of [AuCl(THT)] (0.150 mmol, 0.048 g) dissolved in 2 mL chloroform was added. The addition was done in a dropwise manner. The mixture was stirred at room temperature for 3 min after which two thirds of the solvent was removed in vacuo. The product precipitate was washed with 10 mL diethyl ether (×5) and 10 mL hexane (×3) to remove the displaced THT. The pure product was dried thoroughly in vacuo.

4.4.1. N-(2-(Diphenylphosphino)phenyl)-methylene-butylamine gold(I) chloride (**20**)

To a stirred solution of **5** (0.0518 g, 0.150 mmol) in diethyl ether (5 mL), [AuCl(THT)] (0.048 g, 0.150 mmol) dissolved in chloroform (2 mL) was added. The pure product **20** was obtained as a fine white powder after washing and dried thoroughly in vacuo (0.104 mmol, 0.060 g, 69%). mp: 136–138 °C; ^{1}H NMR: (300 MHz, CDCl3) δ_H 8.53 (s, 1H), 7.80 (dd, J = 7.2 and 4.8 Hz, 1H), 7.60–7.30 (m, 12H), 6.80 (dd, J = 13.1 and 7.7 Hz, 1H), 3.40 (t, J = 6.8 Hz, 2H), 1.21 (m, 2H), 0.93 (sx, J = 7.5 Hz, 2H), and 0.71 (t, J = 7.4 Hz, 3H); ^{13}C NMR: (75 MHz, $CDCl_3$) δ_C 157.7 (d, J = 4.1 Hz), 138.7 (d, J = 6.5 Hz), 134.4 (d, J = 7.5 Hz), 134.1 (d, J = 14.0 Hz), 131.6 (d, J = 8.5 Hz), 131.6, 131.4 (d, J = 2.5 Hz) 129.8 (d, J = 9.9 Hz), 129.0 (d, J = 12.0 Hz), 127.4 (d, J = 56.1 Hz), 60.5, 32.2, 20.3, and 13.7; ^{31}P NMR: (121 MHz, $CDCl_3$) δ_P 32.0; IR: ν_{max} (KBr)/cm^{-1} 2952 and 1653; LRFAB: m/z 578 ($[M+H]^+$, 15%).

4.4.2. N-(2-(Diphenylphosphino)phenyl)-methylene-2-(phenyl) ethylamine gold(I) chloride (**21**)

Phenylethyl amine (0.758 mmol, 0.095 mL) was used as the amine starting material to prepare the iminophosphine intermediate as per the general iminophosphine synthesis (Procedure A) above. To a stirred solution of the pure iminophosphine intermediate (0.059 g, 0.150 mmol) in diethyl ether (5 mL), [AuCl(THT)] (0.048 g, 0.150 mmol) dissolved in chloroform (2 mL) was added. The pure product **21** was obtained as a fine white powder after washing and dried thoroughly in vacuo (0.106 mmol, 0.067 g, 71%). Colourless crystals were obtained from a hexane solution layered with chloroform. mp: 160–162 °C; ^{1}H NMR: (300 MHz, $CDCl_3$) δ_H 8.22 (s, 1H), 7.55 (dd, J = 7.5 and 3.9 Hz, 1H), 7.43–7.24 (m, 11H), 7.17 (t, J = 7.5 Hz, 1H), 7.07–6.96 (m, 3H), 6.81 (d, J = 7.8 Hz, 2H), 6.67 (dd, J = 13.1 and 7.7 Hz, 1H), 3.48 (t, J = 7.7 Hz, 2H), and 2.39 (t, J = 7.7 Hz, 2H); ^{13}C NMR: (75 MHz, $CDCl_3$) δ_C 158.4 (d, J = 3.7 Hz), 139.5, 138.59 (d, J = 6.8 Hz), 134.5 (d, J = 7.1 Hz), 134.1 (d, J = 14.0 Hz), 131.8 (d, J = 8.3 Hz), 131.6, 131.4 (d, J = 2.3 Hz), 130.7, 130.0, 129.8 (d, J = 3.2 Hz), 129.1 (d, J = 11.8 Hz), 128.8, 128.2, 127.6 (d, J = 55.8 Hz), 126.0, 61.8, and 36.7; ^{31}P NMR: (121 MHz, $CDCl_3$) δ_P 32.6; IR: ν_{max} (KBr)/cm^{-1} 3020 and 1644; LRFAB: m/z 591 ($[M-Cl]^+$, 25%). Crystal data are available in the Supplementary Information.

4.4.3. N-(2-(Diphenylphosphino)phenyl)-methylene-benzylamine gold(I) chloride (**22**)

To a stirred solution of **6** (0.057 g, 0.150 mmol) in diethyl ether (5 mL), [AuCl(THT)] (0.048 g, 0.150 mmol) dissolved in chloroform (2 mL) was added. The pure product **22** was obtained as a fine white powder after washing and dried thoroughly in vacuo (0.102 mmol, 0.062 g, 68%). mp: 154–156 °C; ^{1}H NMR: (300 MHz, $CDCl_3$) δ_H 8.69 (s, 1H), 7.90 (dd, J = 7.1 and 4.7 Hz, 1H), 7.59 (t, J = 7.7 Hz, 2H), 7.52–7.33 (m, 13H), 7.17–7.15 (m, 2H), 6.85–6.81 (m, 1H), and 4.68 (s, 2H); ^{13}C NMR: (75 MHz, $CDCl_3$) δ_C 158.5 (d, J = 5.7 Hz), 138.7 (d, J = 7.1 Hz), 137.7, 134.3 (d, J = 5.7 Hz), 134.1 (d, J = 14.0 Hz), 131.6 (d, J = 2.3 Hz), 131.5 (d, J = 2.5 Hz), 131.4 (d, J = 8.3 Hz), 130.1 (d, J = 10.1 Hz), 129.2, 129.1 (d, J = 12.0 Hz), 128.3 (d, J = 9.2 Hz), 127.7 (d, J = 55.8 Hz), 126.8, and 64.0; ^{31}P NMR: (121 MHz, $CDCl_3$) δ_P 30.8; IR: ν_{max} (KBr)/cm^{-1} 3059 and 1631; LRFAB: m/z 612 ($[M+H]^+$, 25%) and 576 ($[M-Cl]^+$, 100%).

4.4.4. N-(2-(Diphenylphosphino)phenyl)-methylene-benzenamine gold(I) chloride (**23**)

To a stirred solution of **7** (0.055 g, 0.150 mmol) in diethyl ether (5 mL), [AuCl(THT)] (0.048 g, 0.150 mmol) dissolved in chloroform (2 mL) was added. The pure product **23** was obtained as a bright green powder after washing and dried thoroughly in vacuo (0.108 mmol, 0.065 g, 72%). This colour is thought to arise from the delocalised π-system that stretches throughout the molecule, enhanced by the unique fluorescent properties that gold is known to exhibit when complexed to certain ligands [72,73]. Green single crystals were grown from a layered solution of dichloromethane, diethyl ether and n-hexane. mp: 187–189 °C; ^{1}H NMR ($CDCl_3$) δ_H 8.53 (s, 1H), 7.87 (dd, J = 6.8 and 4.4 Hz, 1H), 7.50–7.25 (m, 12H), 7.08–7.03 (m, 2H), 6.95 (t, J = 7.4 Hz, 1H), 6.72 (dd, J = 13.2 and 7.8 Hz, 1H), and 6.62 (d, J = 7.5 Hz, 2H); ^{13}C NMR ($CDCl_3$) δ_C 156.5 (d, J = 5.2 Hz), 138.3 (d, J = 6.8 Hz), 134.4 (d, J = 7.1 Hz), 134.1 (d, J = 14.0), 132.2 (d, J = 8.0 Hz), 131.7, 131.6 (d, J = 2.6 Hz), 130.6 (d, J = 10.1 Hz), 130.0, 129.4, 129.1 (d, J = 12.0 Hz), 128.9, 128.3 (d, J = 54.9 Hz), and 126.4; ^{31}P NMR ($CDCl_3$) δ_P 32.0; IR: ν_{max} (KBr)/cm^{-1} 3056 and 1624; LRFAB: m/z 598 ($[M+H]^+$, 21%) and 562 ($[M-Cl]^+$, 38%). Crystal data are available in the Supplementary Information.

4.4.5. (2-Diphenylphosphanyl-benzylidene)-isopropyl-amine gold(I) chloride (**24**)

To a stirred solution of **8** (0.050 g, 0.150 mmol) in diethyl ether (5 mL), [AuCl(THT)] (0.048 g, 0.150 mmol) dissolved in chloroform (2 mL) was added. The pure product **24** was obtained as a fine white powder after washing and dried thoroughly in vacuo (0.104 mmol, 0.058 g, 69%). mp: 172–174 °C; ^{1}H NMR: (300 MHz, CDCl3) δH 8.62 (s, 1H), 7.85–7.81 (dd, J = 6.6 and 4.2 Hz, 1H), 7.63–7.43 (m, 11H), 7.35 (t, J = 7.5 Hz, 1H), 6.80 (dd, J = 13.1 and 7.7 Hz, 1H), 3.40 (p, J = 6.2 Hz, 1H), and 0.95 (d, J = 6.3 Hz, 6H); ^{13}C NMR: (75 MHz, $CDCl_3$) δ_C 155.9 (d, J = 4.6 Hz), 138.8 (d, J = 7.1 Hz), 134.2 (d, J = 8.1 Hz), 134.2 (d, J = 14.0 Hz), 131.7, 131.6, 131.5 (d, J = 2.3 Hz), 130.6, 129.9, 129.7, 129.0 (d, J = 11.9 Hz), 127.2 (d, J = 55.0 Hz), 61.5, and 23.9; ^{31}P NMR: (121 MHz, $CDCl_3$) δ_P 31.7; IR: ν_{max} (KBr)/cm^{-1} 2964 and 1644; LRFAB: m/z 565.4 ($[M+H]^+$, 26%) and 528.4 ($[M-Cl]^+$, 30%).

4.4.6. (2-Diphenylphosphanyl-benzyl)-(2-pyrid-2-yl-ethyl) amine gold(I) chloride (**25**)

To a stirred solution of **9** (0.059 g, 0.150 mmol) in diethyl ether (5 mL), [AuCl(THT)] (0.048 g, 0.150 mmol) dissolved in chloroform (2 mL) was added. The pure product **25** was obtained as a fine white powder after washing and dried thoroughly in vacuo (0.102 mmol, 0.064 g, 68%). mp: 160–162 °C; ^{1}H NMR: (300 MHz, $CDCl_3$) δ_H 8.45 (d, J = 4.5 Hz, 1H), 8.42 (br s, 1H), 7.70 (dd, J = 7.8 and 3.6 Hz, 1H), 7.59–7.41 (m, 11H), 7.33 (t, J = 7.7 Hz, 2H), 7.06–6.98 (m, 2H), 6.82 (dd, J = 13.2 and 7.8 Hz, 1H), 3.80 (t, J = 7.5 Hz, 2H), and 2.80 (t, J =

7.5 Hz, 2H); ^{13}C NMR: (75 MHz, $CDCl_3$) δ_C 159.4, 158.8 (d, J = 3.1 Hz), 149.1, 138.6 (d, J = 6.8 Hz), 136.2, 134.6 (d, J = 6.9 Hz), 134.0 (d, J = 13.7 Hz), 132.0 (d, J = 8.9 Hz), 131.6 (d, J = 2.3 Hz), 131.4 (d, J = 2.3 Hz), 130.8, 130.0 (d, J = 4.1 Hz), 129.8, 129.1 (d, J = 12.0 Hz), 127.6 (d, J = 55.7 Hz), 123.7, 121.2, 59.8, and 38.8; ^{31}P NMR: (121 MHz, $CDCl_3$) δ_P 32.5; IR: ν_{max} (KBr)/cm^{-1} 2835 and 1651; LRFAB: *m/z* 627 ([M + H]$^+$, 4%) and 591 ([M − Cl]$^+$, 31%).

4.4.7. N′-(2-Diphenylphosphanyl-benzylidene)-N,N-dimethyl-propane-1,3-diamine gold(I) chloride (**26**)

To a stirred solution of **10** (0.056 g, 0.150 mmol) in diethyl ether (5 mL), [AuCl(THT)] (0.048 g, 0.150 mmol) dissolved in chloroform (2 mL) was added. The pure product **26** was obtained as a fine white powder after washing and dried thoroughly in vacuo (0.101 mmol, 0.061 g, 67%). mp: 139–141 °C; ^{1}H NMR: (300 MHz, $CDCl_3$) δ_H 8.47 (s, 1H), 7.73 (dd, J = 7.2 and 4.2 Hz, 1H), 7.55–7.32 (m, 11H), 7.27 (t, J = 7.6 Hz, 1H), 6.75 (dd, J = 13.2 and 7.8 Hz, 1H), 3.37 (t, J = 7.1 Hz, 2H), 2.05 (s, 6H), 1.97 (t, J = 7.4 Hz, 2H), and 1.46–1.39 (m, 2H); ^{13}C NMR: (75 MHz, $CDCl_3$) δ_C 158.2 (d, J = 3.8 Hz), 138.6 (d, J = 6.9 Hz), 134.5 (d, J = 7.1 Hz), 134.0 (d, J = 14.0 Hz), 131.8 (d, J = 8.3 Hz), 131.6 (d, J = 2.3 Hz), 131.4 (d, J = 2.3 Hz), 130.7, 129.9, 129.8 (d, J = 4.6 Hz), 129.0 (d, J = 12.0 Hz), 127.4 (d, J = 55.5 Hz), 58.67, 57.16, 45.3, and 28.1; ^{31}P NMR: (121 MHz, $CDCl_3$) δ_P 32.1; IR: ν_{max} (KBr)/cm^{-1} 2937 and 1650; LRFAB: *m/z* 607 ([M + H]$^+$, 87%) and 571 ([M − Cl]$^+$, 62%).

4.4.8. (2-Diphenylphosphanyl-benzylidene)-(2-thiophen-2-yl-ethyl)-amine gold(I) chloride (**27**)

To a stirred solution of **11** (0.060 g, 0.150 mmol) in diethyl ether (5 mL), [AuCl(THT)] (0.048 g, 0.150 mmol) dissolved in chloroform (2 mL) was added. The pure product **27** was obtained as a fine white powder after washing and dried thoroughly in vacuo (0.108 mmol, 0.068 g, 72%). Single crystals were grown from a chloroform solution left at room temperature overnight. Due to the rapid crystallisation process, the crystals obtained are not of exceptionally high quality. mp: 138–140 °C; ^{1}H NMR: (300 MHz, $CDCl_3$) δ_H 8.38 (s, 1H), 7.73 (dd, J = 7.5 and 3.9 Hz, 1H), 7.60–7.39 (m, 10H), 7.34 (t, J = 7.5 Hz, 2H), 7.03 (d, J = 5.1 Hz, 1H), 6.87–6.80 (m, 2H), 6.60 (d, J = 2.4 Hz, 1H), 3.68 (t, J = 7.1 Hz, 2H), and 2.75 (t, J = 7.2 Hz, 2H); ^{13}C NMR: (75 MHz, $CDCl_3$) δ_C 158.8 (d, J = 3.8 Hz), 141.9, 138.4 (d, J = 6.8 Hz), 134.5 (d, J = 7.1 Hz), 133.97 (d, J = 13.7 Hz), 131.9 (d, J = 8.3 Hz), 131.6 (d, J = 2.3 Hz), 131.4 (d, J = 2.5 Hz), 130.4, 129.9 (d, J = 10.1 Hz), 129.8, 129.0 (d, J = 12.0 Hz), 127.5 (d, J = 55.5 Hz), 126.6, 125.0, 123.3, 61.6, and 30.5; ^{31}P NMR: (121 MHz, $CDCl_3$) δ_P 32.3; IR: ν_{max} (KBr)/cm^{-1} 3055 and 1645; LRFAB: *m/z* 596 ([M − Cl]$^+$, 21%) and 487 ([M − C_6H_5S]$^+$, 37%).

4.4.9. tert-Butyl-(2-diphenylphosphanyl-benzylidene)-amine gold(I) chloride (**28**)

To a stirred solution of **12** (0.052 g, 0.150 mmol) in diethyl ether (5 mL), [AuCl(THT)] (0.048 g, 0.150 mmol) dissolved in chloroform (2 mL) was added. The pure product **28** was obtained as a fine white powder after washing and dried thoroughly in vacuo (0.105 mmol, 0.061 g, 70%). Single crystals were grown from chloroform. mp: 192–194 °C; ^{1}H NMR: (300 MHz, $CDCl_3$) δ_H 8.67 (d, J = 1.8 Hz, 1H), 7.86 (ddd, J = 7.6, 4.4 and 1.4 Hz, 1H), 7.61–7.38 (m, 11H), 7.31 (tt, J = 7.7 and 1.7 Hz, 1H), 6.77 (ddd, J = 13.2, 7.8 and 1.2 Hz, 1H), and 0.99 (s, 9H); ^{13}C NMR: (75 MHz, $CDCl_3$) δ_C 153.7 (d, J = 6.5 Hz), 139.3 (d, J = 7.1 Hz), 134.3 (d, J = 12.7 Hz), 134.1 (d, J = 7.1 Hz), 131.7 (d, J = 2.6 Hz), 131.5 (d, J = 2.6 Hz), 131.2 (d, J = 8.6 Hz), 129.7 (d, J = 10.5 Hz), 129.0 (d, J = 12.0 Hz), 127.2 (d, J = 55.1 Hz), 58.6, and 29.6; ^{31}P NMR: (121 MHz, $CDCl_3$) δ_P 31.0; IR: ν_{max} (KBr)/cm^{-1} 2958 and 1644; LRFAB: *m/z* 578 ([M + H]$^+$, 13%) and 542 ([M − Cl]$^+$, 17%).

4.5. General procedure for the preparation of aminophosphine gold(I) complexes (**29**–**35**). Procedure D

[AuCl(THT)] was prepared from literature methods [71]. To a stirred solution of aminophosphine ligand (0.50 mmol) in 20 mL of diethyl ether 0.95 equivalents of [AuCl(THT)] dissolved in 2 mL of chloroform were added. The solution was stirred at room temperature for 5 min. In most cases the product precipitated out of solution within 2 min after addition. When this was not the case, some of the solvent was evaporated in vacuo to ca. 5 mL and the product was precipitated out of the solution by the addition of 10 mL of cold hexane (×3).

4.5.1. N-(2-Diphenylphosphinobenzyl)benzylamine gold(I) chloride (**29**)

The pure aminophosphine ligand **13** (0.50 mmol, 0.191 g) was dissolved in 20 mL of diethyl ether. To this solution a solution of [AuCl(THT)] (0.95 equivalents, 0.475 mmol, 0.152 g) dissolved in chloroform (2 mL) was added. The pure gold complex **29** was obtained as a fine white powder after washing and drying (0.325 mmol, 0.200 g, 65%). mp: 174–177 °C; ^{1}H NMR: (300 MHz, $CDCl_3$) δ_H 7.62 (dd, J = 7.5 and 4.8 Hz, 1H), 7.48–7.33 (m, 11H), 7.19–7.11 (m, 4H), 7.05–7.02 (m, 2H), 6.76 (ddd, J = 11.4, 7.8 and 0.9 Hz, 1H), 4.11 (s, 2H), 3.49 (s, 2H), and 1.43 (br s); ^{13}C NMR: (75 MHz, $CDCl_3$) δ_C 144.2 (d, J = 11.0 Hz), 139.6, 134.2 (d, J = 14.0 Hz), 133.7 (d, J = 7.5 Hz), 131.8–131.7 (m), 130.5 (d, J = 9.0 Hz), 129.6, 129.2 (d, J = 11.6 Hz), 128.7, 128.1 (d, J = 16.0 Hz), 127.4 (d, J = 10.1 Hz), 126.8, 126.7 (d, J = 59.1 Hz), 53.2, and 52.2 (d, J = 11.0 Hz); ^{31}P NMR: (121 MHz, $CDCl_3$) δ_P 26.1; IR: ν_{max} (KBr)/cm^{-1} 3279 and 1433; LRFAB: *m/z* 614 ([M]$^+$, 8%) and 578 ([M − Cl]$^+$, 14%).

4.5.2. N-(2-Diphenylphosphinobenzyl)phenylamine gold(I) chloride (**30**)

The pure aminophosphine ligand **14** (0.50 mmol, 0.184 g) was dissolved in 20 mL of diethyl ether. To this solution a solution of [AuCl(THT)] (0.95 equivalents, 0.475 mmol, 0.152 g) dissolved in chloroform (2 mL) was added. The pure gold complex **30** was obtained as a blue powder after washing and drying (0.405 mmol, 0.243 g, 81%). The formation of two crystal forms was possible. In the first, the free base **30** could be crystallised to form crystals **30a** as the neutral gold(I) complex from a layered solution of diethyl ether and hexane. In contrast, if **30** was first treated with aqueous HCl, **30b** as the hydrochloride salt crystal form could be produced from a layered solution of chloroform and *n*-heptane. For compound **30**: mp: 223–225 °C; ^{1}H NMR: (300 MHz, $CDCl_3$) δ_H 7.60 (m, 1H), 7.52–7.39 (m, 11H), 7.17 (m, 1H), 6.94 (t, J = 7.5 Hz, 2H), 6.77 (dd, J = 13.1 and 7.7 Hz, 1H), 6.57 (t, J = 7.2 Hz, 1H), 6.17 (d, J = 7.8 Hz, 2H), and 4.61 (s, 2H); ^{13}C NMR: (75 MHz, $CDCl_3$) δ_C 146.7, 143.3, 134.4 (d, J = 13.7 Hz), 133.7 (d, J = 7.4 Hz), 132.1 (d, J = 2.6 Hz), 132.1, 129.3 (d, J = 12.0 Hz), 129.1, 129.0, 128.4, 127.5 (d, J = 9.2 Hz), 127.3, 126.1 (d, J = 57.5 Hz), 118.0, 112.8, and 47.6 (d, J = 12.6 Hz); ^{31}P NMR: (121 MHz, $CDCl_3$) δ_P 25.7; IR: ν_{max} (KBr)/cm^{-1} 3414 and 1435; LRFAB: *m/z* 564.5 ([M − Cl]$^+$, 33%). Crystal data for the neutral gold(I) complex **30a** and the gold(I) hydrochloride salt **30b** are available in the Supplementary Information.

4.5.3. (2-Diphenylphosphanyl-benzyl)-isopropyl-amine gold(I) chloride (**31**)

The synthesis and structure of **31** have already been published [44].

4.5.4. (2-Diphenylphosphanyl-benzyl)-pyrid-2-ylmethyl-amine gold(I) chloride (**32**)

The structure of **32** has already been published [47].

4.5.5. (2-Diphenylphosphanyl-benzyl)-(2-pyrid-2-yl-ethyl)-amine gold(I) chloride (**33**)

The pure aminophosphine ligand **17** (0.50 mmol, 0.198 g) was dissolved in 20 mL of diethyl ether. To this solution a solution of [AuCl(THT)] (0.95 equivalents, 0.475 mmol, 0.152 g) dissolved in

chloroform (2 mL) was added. The pure gold complex **33** was obtained as a fine brown powder after washing and drying (0.315 mmol, 0.198 g, 63%). mp: 135–136 °C; ^{1}H NMR: (300 MHz, $CDCl_3$) δ_H 8.43 (dd, J = 6.0 and 1.8 Hz, 1H), 7.63 (dd, J = 6.6 and 5.4 Hz, 1H), 7.57–7.40 (m, 11H), 7.20 (t, J = 7.5 Hz, 2H), 7.08–7.04 (m, 2H), 6.79 (dd, J = 12.8 and 7.7 Hz, 1H), 4.15 (s, 2H), 2.84 (t, J = 6.9 Hz, 2H), 2.72 (t, J = 6.6 Hz, 2H), and 1.83 (br s); ^{13}C NMR: (75 MHz, $CDCl_3$) δ_C 159.9, 149.0, 143.9 (d, J = 12.8 Hz), 136.4, 134.2 (d, J = 14.0 Hz), 133.8 (d, J = 7.4 Hz), 131.9–131.8 (m), 130.4 (d, J = 9.2 Hz), 129.6, 129.2 (d, J = 12.0 Hz), 128.7, 127.4 (d, J = 9.4 Hz), 126.6 (d, J = 59.2 Hz), 123.5, 121.2, 52.5, 48.6, and 37.4; ^{31}P NMR: (121 MHz, $CDCl_3$) δ_P 26.1; IR: ν_{max} (KBr)/cm^{-1} 3283 and 1435; LRFAB: *m/z* 593 ($[M-Cl]^+$, 25%).

4.5.6. N′-(2-Diphenylphosphanyl-benzyl)-N,N-dimethyl-propane-1,3-diamine gold(I) chloride (**34**)

The pure aminophosphine ligand **18** (0.50 mmol, 0.188 g) was dissolved in 20 mL of diethyl ether. To this solution a solution of [AuCl(THT)] (0.95 equivalents, 0.475 mmol, 0.152 g) dissolved in chloroform (2 mL) was added. The pure gold complex **34** was obtained as a viscous yellow oil (0.240 mmol, 0.146 g, 48%). ^{1}H NMR: (300 MHz, $CDCl_3$) δ_H 7.57 (dd, J = 7.4 and 4.6 Hz, 1H), 7.52–7.35 (m, 11H), 7.15 (t, J = 7.7 Hz, 1H), 6.73 (dd, J = 12.8 and 8.0 Hz, 1H), 4.05 (s, 2H), 2.37 (t, J = 7.2 Hz, 2H), 2.11–2.07 (m, 8H), 1.67 (br s), and 1.30 (p, J = 7.2 Hz, 2H); ^{13}C NMR: (75 MHz, $CDCl_3$) δ_C 144.4 (d, J = 10.8 Hz), 134.1 (d, J = 14.0 Hz), 133.6 (d, J = 7.4 Hz), 131.7 (d, J = 2.3 Hz), 130.3 (d, J = 9.1 Hz), 129.7, 129.1 (d, J = 11.9 Hz), 128.8, 127.2 (d, J = 9.9 Hz), 126.5 (d, J = 58.7 Hz), 57.7, 53.1 (d, J = 10.9 Hz), 48.0, 45.4, and 27.5; ^{31}P NMR: (121 MHz, $CDCl_3$) δ_P 26.2; IR: ν_{max} (NaCl)/cm^{-1} 2817 and 1437; LRFAB: *m/z* 609 ($[M+H]^+$, 20%) and 573 ($[M-Cl]^+$, 23%).

4.5.7. N-(2-Diphenylphosphanyl-benzyl)-(2-thiophen-2-yl-ethyl)-amine gold(I) chloride (**35**)

The pure aminophosphine ligand **19** (0.50 mmol, 0.184 g) was dissolved in 20 mL of diethyl ether. To this solution a solution of [AuCl(THT)] (0.95 equivalents, 0.475 mmol, 0.152 g) dissolved in chloroform (2 mL) was added. The pure gold complex **35** was obtained as a fine white powder (0.335 mmol, 0.212 g, 67%). ^{1}H NMR: (300 MHz, $CDCl_3$) δ_H 7.55–7.35 (m, 11H), 7.16 (t, J = 7.1 Hz, 2H), 7.01 (dd, J = 5.4 and 1.2 Hz, 1H), 6.81–6.72 (m, 2H), 6.59 (d, J = 3.3 Hz, 1H), 4.10 (s, 2H), 2.59 (d, J = 3.3 Hz, 4H), and 1.21 (br s); ^{13}C NMR: (75 MHz, $CDCl_3$) δ_C 144.3 (d, J = 10.9 Hz), 142.3, 134.2 (d, J = 13.7 Hz), 133.9 (d, J = 7.1 Hz), 131.7 (d, J = 2.6 Hz), 130.4 (d, J = 9.1 Hz), 129.9, 129.2 (d, J = 11.9 Hz), 129.1, 127.4 (d, J = 10.0 Hz), 126.7, 126.7 (d, J = 58.9 Hz), 125.0, 123.4, 52.9 (d, J = 10.2 Hz), 50.5, and 29.9; ^{31}P NMR: (121 MHz, $CDCl_3$) δ_P 26.3; IR: ν_{max} (KBr)/cm^{-1} 3053 and 1435; LRFAB: *m/z* 634 ($[M+H]^+$, 6%) and 598 ($[M-Cl]^+$, 25%).

4.6. Crystallographic structure determination

The intensity data for all compounds were collected at 173 K on a Bruker SMART 1K CCD diffractometer with area detector using graphite monochromated Mo–K_α radiation (λ = 0.71073 Å, 50 kV, 30 mA). Data reduction was carried out using the program *SAINT+* [73] and face indexed absorption corrections were made using the program *XPREP* [74]. The structures were solved by direct methods using *SHELXTL* [75]. Non-hydrogen atoms were first refined isotropically followed by anisotropic refinement by full matrix least-squares calculations based on F^2 using *SHELXTL*. Hydrogen atoms were first located in the difference map then positioned geometrically and allowed to ride on their respective parent atoms. Diagrams and publication material were generated using SHELXTL and Mercury [76]. Selected bond lengths and angles for compounds **4**, **14**, **21**, **23**, **30a** and **30b** are summarised in Table 1 in comparison to triphenylphosphine gold(I) chloride ($AuClPPh_3$; **36**).

4.7. Cell lines and culture conditions

3T3 (mouse embryonic fibroblast) cells and CHO (Chinese hamster ovary) cells were obtained from the Sir William Dunn School of Pathology, University of Oxford, South Parks Road, Oxford, United Kingdom. A549J (human lung adenocarcinoma epithelial) cells, Caski (human cervical cancer) cells, HepG2 (human hepatocellular liver carcinoma) cells, HeLa (human cervical adenocarcinoma) cells, Hek 293-T (human embryonic kidney) cells, HT-29 (human colon adenocarcinoma grade II) cells, H157 (human non-small cell lung carcinoma) cells, Jurkat T (human leukaemia) cells, MCF7 (human breast adenocarcinoma) cells, MG-63 (human osteogenic sarcoma) cells and KMST-6 (non-cancer human fibroblast) cells were kindly provided by Prof D. Hendricks, Department of Clinical and Laboratory Medicine, University of Cape Town, South Africa. Cells were cultured in CELLSTAR® Cell Culture Flasks (Greiner Bio-One GmbH, Frickenhausen, Germany). All cell culture reagents were obtained from Invitrogen Ltd. (Carlsbad, California, USA). Jurkat T cells were cultured in Roswell Park Memorial Institute (RPMI) medium; CHO cells were cultured in Ham's F12 nutrient mixture; all other cell lines were cultured in Dulbecco's Minimal Essential Medium (DMEM). The cell culture medium for all cell lines was supplemented with 10% heat-inactivated foetal calf serum, 1 mM sodium pyruvate, 2 mM L-glutamine and 1% Penicillin/Streptomycin. Cultures were maintained at 37 °C in a humidified atmosphere containing 5% CO_2 and 95% air.

4.8. Cytotoxicity tests in cell lines

Cell proliferation was determined using the MTT assay following methods previously described [49–53]. Specifically, adherent cells were trypsinised and both adherent and suspension cells were plated in 96-well cell culture plates (24 000 cells per well; 100 μL/well) and cultured at 37 °C in a humidified CO_2 incubator until 90% confluence was reached. The culture medium was removed and replaced with 100 μL of fresh medium, which contained various concentrations of the test compounds (ranging from 10 μM to 100 μM). As a positive control, cells were treated with 100 μM cisplatin, for all cell lines used in this study. All treatments were performed in triplicate. The cells were incubated at 37 °C in a humidified CO_2 incubator for 20 h. After incubation, 10 μL of a 5 mg/mL solution of MTT was added to each well and the plates were incubated for a further 4 h at 37 °C. At the end of the 24 hour incubation period, the media was removed and DMSO (100 μL) was added to each well. The plates were placed on a rotating shaker for 10 min, and the optical density (OD) was determined at 560 nm using a LabSystems Multiscan Plus microplate reader. Cell viability was determined using the following formula: (Viable cells)% = (OD560 of drug-treated sample/OD560 of untreated sample) × 100. IC_{50} values (the half maximal inhibitory concentration) were calculated using Graph Pad Prism (GraphPad Software, Inc.). Triplicate experiments were conducted and the results were expressed as mean ± SD.

4.9. APOPercentage™ apoptosis assay

The assay was performed as described in the literature [54]. In brief, the cells were plated in 24 well cell culture plates at a cell density of 2.5×10^4 cells/mL and incubated for 24 h at 37 °C in a humidified CO_2 incubator. The cells were treated for 24 h with the test compounds at 50 μM concentrations. Stock solutions of the compounds were prepared in DMSO and working concentrations were prepared in cell culture media. The final DMSO concentration in the treated wells was less than 0.1%. Following the 24 hour treatment, the cells were recovered by trypsinisation and stained with APOP*ercentage*™ dye. The cells were analysed on a FACScan™ (Becton Dickson) instrument equipped with a 488 nm argon laser. APOP*ercentage*™ fluorescence was measured using the FL3 channel.

Acknowledgements

We thank Mintek, the University of Johannesburg and the University of the Western Cape for financial support and permission to publish the results.

Appendix A. Supplementary data

Supplementary data to this article can be found online at http://dx.doi.org/10.1016/j.jinorgbio.2015.01.014 including X-ray crystallographic data in CIF format for **4**, **14**, **21**, **23**, **30a** and **30b**; crystal data and structure refinement data for **4**, **14**, **21**, **23**, **30a** and **30b**; mercury diagrams for **4**, **21**, **23**, **30a** and **30b**. Sets of NMR spectra are provided for selected compounds.

Crystallographic data have been deposited with the Cambridge Crystallographic Data Centre as CCDC 1009263; CCDC 1009264; CCDC 1009265; CCDC 1009266; CCDC 1009267 and CCDC 1009268 for **4**, **14**, **21**, **23**, **30a** and **30b**, respectively. Copies of data can be obtained, free of charge, upon application to CCDC, 12 Union Road, Cambridge CB2 1EZ, U.K. (deposit@CCDC.com.ac.uk).

References

[1] H.S. Youn, J.Y. Lee, S.I. Saitoh, K. Miyake, D.H. Hwang, Biochem. Biophys. Res. Commun. 350 (2006) 866–871.
[2] K.P. Bhabak, B.J. Bhuyan, G. Mugesh, Dalton Trans. 40 (2011) 2099–2111.
[3] L. Messori, G. Marcon, Met. Ions Biol. Syst. 41 (2004) 279–304.
[4] S.S. Gunatilleke, A.M. Barrios, J. Med. Chem. 49 (2006) 3933–3937.
[5] S.L. De Wall, C. Painter, J.D. Stone, R. Bandaranayake, D.C. Wiley, T.J. Mitchison, L.J. Stern, B.S. DeDecker, Nat. Chem. Biol. 2 (2006) 197–201.
[6] Y. Omata, M. Folan, M. Shaw, R.L. Messer, P.E. Lockwood, D. Hobbs, S. Bouillaguet, H. Sano, J.B. Lewis, J.C. Wataha, Toxicol. In Vitro 20 (2006) 882–890.
[7] R. Rubbiani, I. Kitanovic, H. Alborzinia, S. Can, A. Kitanovic, L.A. Onambele, M. Stefanopoulou, Y. Geldmacher, W.S. Sheldrick, G. Wolber, A. Prokop, S. Woelfl, I. Ott, J. Med. Chem. 53 (2010) 8608–8618.
[8] A. De Luca, C.G. Hartinger, P.J. Dyson, M. Lo Bello, A. Casini, J. Inorg. Biochem. 119 (2013) 38–42.
[9] Y. Wang, M. Liu, R. Cao, W. Zhang, M. Yin, X. Xiao, Q. Liu, N. Huang, J. Med. Chem. 56 (2013) 1455–1466.
[10] K. Nam-Hoon, P. Hyo Jung, O. Mi-Kyung, K. In-Sook, BMB Rep. 46 (2013) 59–64.
[11] J.M. Madeira, D.L. Gibson, W.F. Kean, A. Klegeris, Inflammopharmacology 20 (2012) 297–306.
[12] S.J. Berners-Price, A. Filipovska, Metallomics 3 (2011) 863–873.
[13] E.A. Pacheco, E.R.T. Tiekink, M.W. Whitehouse, Biomedical applications of gold and gold compounds, in: C. Corti, R. Holliday (Eds.), Gold: Science and Applications, CRC Press, Boca Raton, 2010, pp. 217–230.
[14] L. Messori, F. Abbate, G. Marcon, P. Orioli, M. Fontani, E. Mini, T. Mazzei, S. Carotti, T. O'Connell, P. Zanello, J. Med. Chem. 43 (2000) 3541–3548.
[15] G. Marcon, S. Carotti, M. Coronnello, L. Messori, E. Mini, P. Orioli, T. Mazzei, M.A. Cinellu, G. Minghetti, J. Med. Chem. 45 (2002) 1672–1677.
[16] A. Casini, M.A. Cinellu, G. Minghetti, C. Gabbiani, M. Coronnello, E. Mini, L. Messori, J. Med. Chem. 49 (2006) 5524–5531.
[17] C.F. Shaw III, Chem. Rev. 99 (1999) 2589–2600 (and references cited therein).
[18] D.T. Felson, J.J. Anderson, R.F. Meenan, Arthritis Rheum. 33 (1990) 1449–1461.
[19] E.A. Pacheko, E.R.T. Tiekink, M.W. Whitehouse, Gold compounds and their application in medicine, in: F. Mohr (Ed.), Gold Chemistry: Applications and Future Directions in the Life Sciences, Wiley-ACH, Weinheim, 2009, p. 284.
[20] A.L. Balch, T.Y. Garcia, A primer of gold chemistry, in: C. Corti, R. Holliday (Eds.), Gold: Science and Applications, CRC Press, Boca Raton, 2010, pp. 35–42.
[21] A.R. Latham, V.C. Hascall, H.B. Gray, Inorg. Chem. 4 (1965) 788–792.
[22] L. Cattalini, A. Orio, M.L. Tobe, J. Am. Chem. Soc. 89 (1967) 3130–3134.
[23] K.J. Kilpin, W. Henderson, Chem. N. Z. 73 (2009) 102–105.
[24] C. Gabbiani, A. Casini, L. Messori, Gold Bull. 40 (2007) 73–88.
[25] M. Howe-Grant, K.C. Wu, W.R. Bauer, S.J. Lippard, Biochemistry 15 (1976) 4339–4346;
R.J. Knox, F. Friedlos, D.A. Lydall, J. Roberts, Cancer Res. 46 (1986) 1972–1979.
[26] C. Gabbiani, L. Messori, Anticancer Agents Med. Chem. 11 (2011) 929–939.
[27] A. Casini, C. Hartinger, C. Gabbiani, E. Mini, P.J. Dyson, B.K. Keppler, L. Messori, J. Inorg. Biochem. 102 (2008) 564–575.
[28] J.C. Lima, L. Rodriguez, Anticancer Agents Med. Chem. 11 (2011) 921–928.
[29] A. Casini, L. Messori, Curr. Topics Med. Chem. 11 (2011) 2647–2660.
[30] G. Droga-Mazovec, L. Bojič, A. Petelin, S. Ivanova, R. Romih, U. Repnik, G.S. Salvesen, V. Stoka, V. Turk, B.J. Turk, Biol. Chem. 283 (2008) 19140–19150.
[31] S. Gunatilleke, C.A. De Oliveira, J.A. McCammon, A.M. Barrios, J. Biol. Inorg. Chem. 13 (2008) 555–561.
[32] S.S. Gunatilleke, A.M. Barrios, J. Inorg. Biochem. 102 (2008) 555–563.
[33] A. Bindoli, M.P. Rigobello, G. Scutari, C. Gabbiani, A. Casini, L. Messori, Coord. Chem. Rev. 253 (2009) 1692–1707.
[34] B.M. Wile, R.J. Burford, R. McDonald, M.J. Ferguson, M. Stradiotto, Organometallics 25 (2006) 1028–1035.
[35] R.C.J. Atkinson, V.C. Gibson, N.J. Long, Chem. Soc. Rev. 33 (2004) 313–328.
[36] P.J. Guiry, C.P. Saunders, Adv. Synth. Catal. 346 (2004) 497–537.
[37] C. Muller, R.J. Lachicotte, W.D. Jones, Organometallics 21 (2002) 1118–1123.
[38] D.B.G. Williams, M. Pretorius, J. Mol. Catal. A Chem. 284 (2008) 77–84.
[39] J. Andrieu, J.M. Camus, P. Richard, R. Poli, L. Gonsalvi, F. Vizza, M. Peruzzini, Eur. J. Inorg. Chem. 1 (2006) 51–61.
[40] E.J. Zijp, J.I. Van der Vlugt, D.M. Tooke, A.L. Spek, D. Vogt, J. Chem. Soc. Dalton Trans. 3 (2005) 512–517.
[41] A. Habtemariam, P.J. Sadler, Chem. Commun. 15 (1996) 1785–1786.
[42] A. Habtemariam, J.A. Parkinson, N. Margiotta, T.W. Hambley, S. Parsons, P.J. Sadler, Dalton Trans. 4 (2001) 362–372.
[43] R.J. Bowen, M.A. Fernandez, P.W. Gitari, M. Layh, R.M. Moutloali, Eur. J. Inorg. Chem. 10 (2005) 1955–1963.
[44] D.B.G. Williams, T. Traut, F.H. Kriel, W.E. Van Zyl, Inorg. Chem. Commun. 10 (2007) 538–542.
[45] D.B.G. Williams, H. Lombard, C.W. Holzapfel, Synth. Commun. 31 (2001) 2077–2081;
D.B.G. Williams, M. Ajam, A. Ranwell, Organometallics 26 (2007) 4692–4695;
D.B.G. Williams, K. Blann, J. Caddy, Org. Prep. Proc. Int. 33 (2001) 565–602.
[46] N.C. Baenziger, W.E. Bennett, D.M. Soboroff, Acta Crystallogr. B32 (1976) 962–963.
[47] T. Traut, F.H. Kriel, W.E. Van Zyl, D.B.G. Williams, Acta Crystallogr. E 67 (2001) (m1625-m1625).
[48] H. Chiririwa, J.R. Moss, D. Hendricks, G.S. Smith, R. Meijboom, Polyhedron 49 (2013) 29–35.
[49] T. Mossman, J. Immunol. Methods 65 (1983) 55–63.
[50] Y. Eguchi, S. Shimizu, Y. Tsujimoto, Cancer Res. 57 (1997) 1835–1840.
[51] F.M. Freimoser, C.A. Jacob, M. Aebi, U. Tuor, Appl. Environ. Microbiol. 65 (1999) 3727–3729.
[52] D. Gerlier, N. Thomasset, J. Immunol. Methods 94 (1986) 57–63.
[53] P.W. Sylvester, Methods Mol. Biol. 716 (2011) 157–168.
[54] M. Meyer, M. Essack, S. Kanyanda, J.G. Rees, Biotechniques 45 (2008) 317–320.
[55] J.A. Lessa, J.C. Guerra, L.F. de Miranda, C.F. Romeiro, J.G. Da Silva, I.C. Mendes, N.L. Speziali, E.M. Souza-Fagundes, H. Beraldo, J. Inorg. Biochem. 105 (2011) 1729–1739.
[56] L.R. Gouvea, L.S. Garcia, D.R. Lachter, P.R. Nunes, F. De Castro Pereira, E.P. Silveira-Lacerda, S.R. Louro, P.J. Barbeira, L.R. Teixeira, Eur. J. Med. Chem. 55 (2012) 67–73.
[57] M. Baron, S. Bellamin-Laponnaz, C. Tubaro, M. Basato, S. Bogialli, A. Dolmella, J. Inorg. Biochem. 141 (2014) 94–102.
[58] L. Boselli, I. Ader, M. Carraz, C. Hemmert, O. Cuvillier, H. Gornitzka, Eur. J. Med. Chem. 85 (2014) 87–94.
[59] E. García-Moreno, S. Gascón, E. Atrián-Blasco, M.J. Rodriguez-Yoldi, E. Cerrada, M. Laguna, Eur. J. Med. Chem. 79 (2014) 164–172.
[60] C. Liu, Z. Liu, M. Li, X. Li, Y.-S. Wong, S.-M. Ngai, W. Zheng, Y. Zhang, T. Chen, PLoS One 8 (1) (2013) e53945.
[61] D. Hanahan, R.A. Weinberg, Cell 144 (2011) 646–674.
[62] A. Russo, M. Terrasi, V. Agnese, D. Santini, V. Bazan, Ann. Oncol. (Suppl. 7) (2006) 115–123.
[63] J. Weyermanna, D. Lochmanna, A. Zimmer, Int. J. Pharm. 288 (2005) 369–376.
[64] R.H. Shoemaker, Nat. Rev. Cancer 6 (2006) 813–823.
[65] N.A. Berger, G. Weber, J. Natl. Cancer Inst. 58 (1977) 1167–1169.
[66] C.P. Anderson, J.M. Tsai, W.E. Meek, R.M. Liu, Y. Tang, H.J. Forman, C.P. Reynolds, Exp. Cell Res. 246 (1999) 183–192.
[67] D.L. Pavia, G.M. Lampman, G.S. Kriz, Introduction to Spectroscopy, Saunders College Publishing, New York, 1996. 116.
[68] D.D. Perrin, W.L.F. Armarego, Purification of Laboratory Chemicals, Pergamon Press, Oxford, 1988.
[69] D.B.G. Williams, M. Lawton, J. Org. Chem. 75 (2010) 8351–8354.
[70] E. Shirakawa, H. Yoshida, H. Takaya, Tetrahedron Lett. 38 (1997) 3759–3762.
[71] R. Usón, A. Laguna, M. Laguna, Inorg. Synth. 26 (1989) 85–91.
[72] A.L. Balch, Struct. Bond. 123 (2007) 1–40.
[73] K.M.-C. Wong, V.W.-W. Yam, RSC Polym. Chem. Ser. 2 (2012) 245–286.
[74] Bruker, SAINT+. Version 6.02(includes XPREP and SADABS) Bruker AXS Inc., Madison, Wisconsin, USA, 1999.
[75] Bruker, SHELXTL. Version 5.1(includes XS, XL, XP, XSHELL) Bruker AXS Inc., Madison, Wisconsin, USA, 1999.
[76] C.F. Macrae, P.R. Edgington, P. McCabe, E. Pidcock, G.P. Shields, R. Taylor, M. Towler, J. Van de Streek, J. Appl. Crystallogr. 39 (2006) 453–457.